"An empirical constitutive flow equation for polycarbonate deformed in simple shear was derived."

The Plane Simple Shear Testing of Polycarbonate

by
Adolfo Jesus R. Gopez, Ph.D.

ABSTRACT

The plane simple shear test is applied to the case of polycarbonate, an amorphous polymer with a number average molecular weight of 15,600 g/mole and a degree of polydispersity of 1.85. At room temperature, when polycarbonate is in the glassy state (T_g = 145°C), the shear stress-shear strain curve can be divided into five stages. Stage I is characterized by an almost linear variation of the shear stress with the shear strain, and a gradual diminution of the slope towards the end of the stage. Stage II corresponds to a drop in the shear stress even as the shear strain increases, while a linear portion of the curve with a small positive slope constitutes Stage III. A steeper portion of the curve corresponds to Stage IV. Towards the end of the latter stage, the slope of the curve decreases. In Stage V, a progressive reduction of the slope indicates the onset of rupture and a sudden drop in the stress level indicates the end of the test. The yield point has been shown to correspond with the end of Stage I, and microscopic investigation indicates that a shear band forms during Stage II. The band, which is initially short and narrow (0.1 mm), grows in length during Stage II and widens during Stage III. The slope change between Stages III and IV indicates that the band occupies the entire calibrated part of the specimen..

The effects of temperature and strain rate on the shear response was investigated. At low temperatures the stress drop disappeared and a rigid behavior was observed, while at temperatures around and above Tg, a rubbery (elastomeric) response was observed. The strain rate had a weaker although significant effect. Increasing the strain rate increased the observed stress levels. Reversal of the loading mode showed a reduced flow stress and the disappearance of the stress drop at yield.

Using the test data, an empirical constitutive flow equation for polycarbonate deformed in simple shear was derived. A multiplicative law separating the effects of the different variables was shown to fit the data. A mechanism of plastic deformation based on the nucleation and propagation of defects was proposed and an attempt was made to compare the shear test curve with that of a uniaxial tensile test for polycarbonate using the concepts of equivalent stress and strain. Results of the comparison indicate that these tests cannot yet be derived from each other and that perhaps a better understanding of the basic mechanisms of plastic deformation in glassy amorphous polymers could lead to a more meaningful comparison of the tests.

INTRODUCTION

Amorphous polymers in their glassy state show evidence of extensive plastic deformation. Conventional materials testing methods applied to polymers (such as tensile and compression tests) indicate the presence of different phenomena which occur together with the onset of plastic deformation and tend to obscure the observation of the latter process. In particular, the formation of intersecting deformation bands (Bauwens, 1967; Argon et. al., 1968) and localized or diffused necking of test specimens (Brown and Ward, 1968; G'sell and Jonas, 1979) may be cited. These phenomena are often accompanied by rapid transitory variations in the measured stresses such as stress drops at yield points and stress overshoots during strain rate changes. To further complicate the situation, artifacts such as crazing (Kramer, 1982), kinking and folding in compression and brittle fracture (Bowden and Jukes, 1968) have also been observed to mask the effects of plastic deformation. A test method which suppresses these phenomena would therefore be highly desirable.

The mechanisms of plastic deformation in glassy amorphous polymers and in (amorphous) metallic glasses (see for example Escaig and G'sell, 1982) have yet to be defined. The models which have been proposed for amorphous polymers (Robertson, 1966; Argon, 1973; Bowden and Raha, 1974) visualized elementary deformation mechanisms as being controlled by macromolecular mobility and interaction. The comparison and confrontation of these models with experimental data have so far been difficult due to the masking effects already cited.

The possibility of using other testing methods to obtain supplementary data now arises. The torsion test offers a possibility (Wu and Turner, 1973) but due to its complex deformation geometry, the interpretation of its results can prove to be difficult (Canova et. al., 1982). An alternative would be the plane simple shear test developed by Boni (1981) and G'sell et. al. (1983).

Initial results obtained from the application of the plane simple shear test to polyethylene, a semi-crystalline polymer, are encouraging from the standpoint of suppression of crazing or necking phenomena during plasticity (Boni, 1981; G'sell et. al., 1983). The application of this testing method to an amorphous glassy polymer could lead to useful supplementary data and observations. Polycarbonate, an amorphous polymer with very little tendency to crystallize and a high glass transition temperature ($T_g = 145°C$), was chosen for testing.

This study has three objectives. Initially testing will be carried out under different conditions in order to obtain an empirical constitutive flow equation for polycarbonate in simple shear. The results will then be analyzed to obtain relevant information regarding the elementary mechanisms of plastic deformation. Finally, a comparison between the shear test and the tensile test will be done to see if the results of one test can be derived from the others.

EXPERIMENTAL PROCEDURE

Material

The material used in this study is a commercial grade bisphenol A polycarbonate (Makrolon). Figure 1 shows the structure of the monomer (Heijboer, 1969; Miles and Briston, 1965). The principal chain of the monomer contains two phenyl rings connected by a central carbon atom. One end of the monomer has a carbonate radical while the side groups linked to the central carbon are methyl radicals. The molecular weight of a monomer is 254 g/mole.

This polymer is obtained by the phosgenation of bisphenol. A, resulting in linear molecules (Miles and Briston, 1965). It is non-reticulated (no cross linking) and can be considered as a linear polyester of carbonic acid.

Gel permeation chromatography showed that the number average molecular weight $\overline{M}n$ = 15600 g/mole while the weight average molecular weight $\overline{M}w$ is 28800 g/mole. This gives a degree of polydispersity $\overline{M}w/\overline{M}n$ of 1.85 for this polymer. Based on the number average molecular weight, the average degree of polymerization is 60 monomers per molecule.

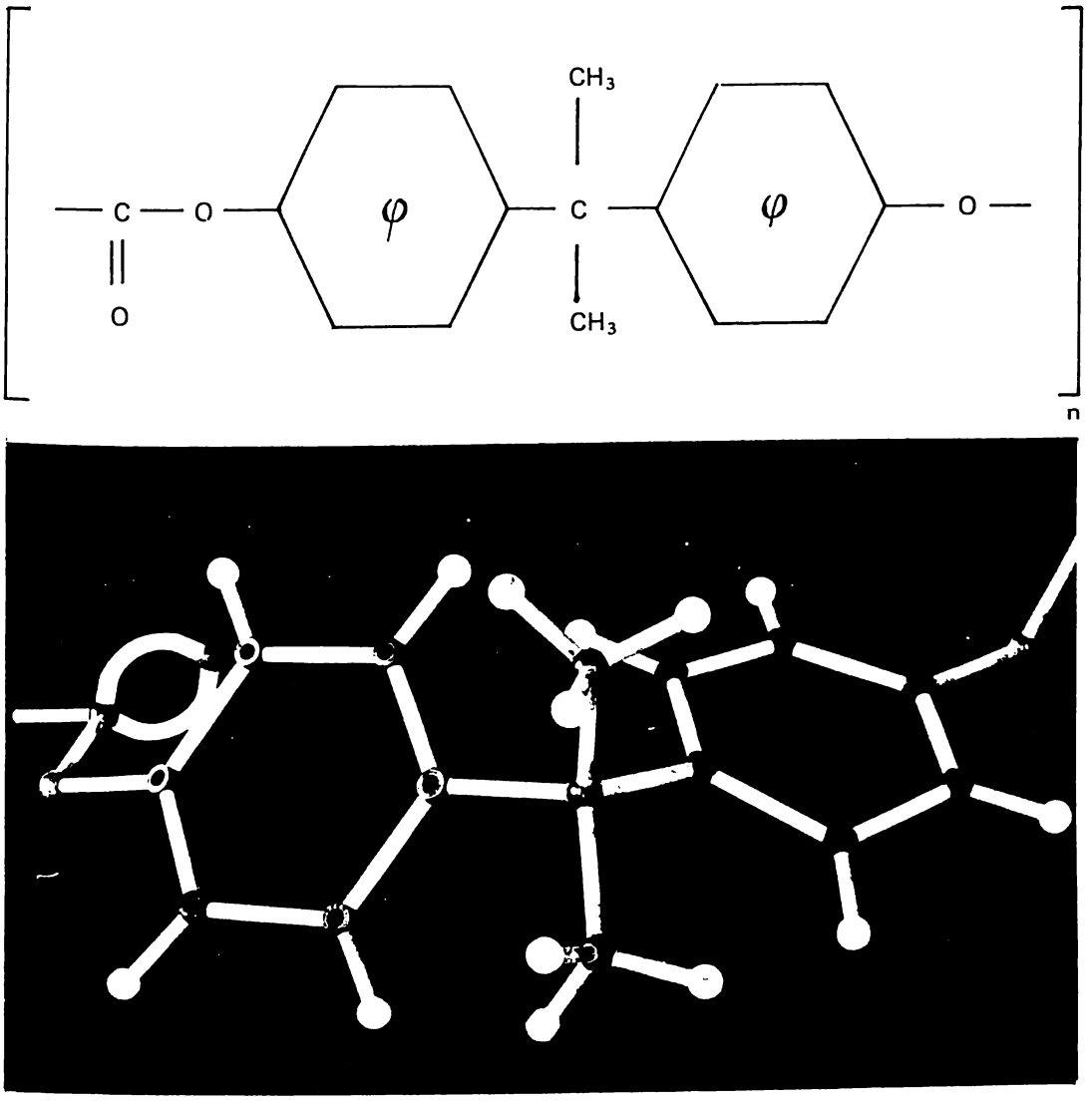

Figure 1: Structure of Bisphenol A Polycarbonate Monomer molecular weight = 254

Some other physical properties of this polycarbonate are given in the following table:

Density (23°C)	1.1974 ± 0.0013 g/cm^3	
Index of Refraction	1.586	DIN 53491
Coefficient of Transmission (Visible light)	0.85	DIN 5036
Young's Modulus	2200 MPa	DIN 53457

The density was determined using a specific gravity column filled with a mixture of liquids giving varying densities with position in the column. The index of refraction of undeformed polycarbonate and the coefficient of transmission of visible light and Young's modulus were obtained from manufacturer's data (Bayer-Rohm). The standard DIN tests used to measure the properties are given in the third column.

Figure 2 shows the curve obtained by wide-angle X-ray diffraction. A principal peak can be seen at $\theta = 5°$ with a secondary peak at around 13°. This type of curve indicates that the material is amorphous (Kakudo and Kasai, 1972). If the material had a non-negligible crystalline phase, additional strong peaks should have been present corresponding to

diffraction by the crystallographic planes in the crystallites. The absence of these peaks indicates that the polycarbonate used in this study can be considered to be essentially amorphous.

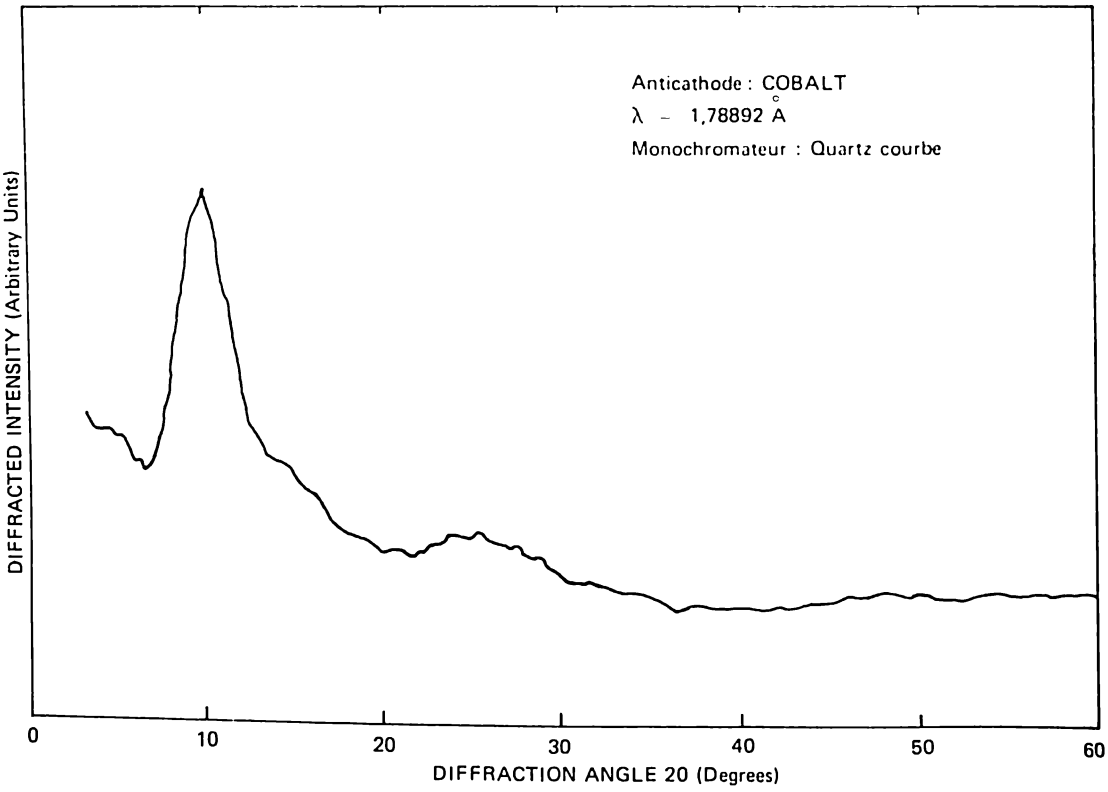

Figure 2: Wide angle X-ray diffraction diagram of undeformed polycarbonate

Data from dynamic mechanical testing of Makrolon has been published in the literature (Heijboer, 1969 and 1977). The glass transition temperature of this polymer has been shown to be 145°C (Heijboer, 1977). At ambient temperature, polycarbonate is therefore in the glassy state.

The material was received in the form of 9-mm thick extruded plates. The low initial birefringence value, about $5\ 10^{-5}$, indicated that the manufacturing process had imparted very little molecular orientation

Testing Methods

THE PLANE SIMPLE SHEAR TEST

Principle of the Test

The plane simple shear test developed by Boni (1981) and G'sell et. al. (1983) was used in this study. The simple shear testing apparatus and its mode of operation have been described in detail in the publications just cited. Consequently only an overview of test's principal characteristics will be given in this section.

Figure 3 shows a parallelepiped solid undergoing simple shear deformation. Planes in the solid which are normal to the Ox_2 axis are translated parallel to the shear direction Ox_1. No deformation takes place along Ox_3 and the solid is thus subjected to plane strain conditions. No volume change takes place during the deformation. The shear strain γ is conventionally defined as the ratio x/h (Dieter, 1976), with x being the relative displacement in the deformed solid and h being the sheared width or the distance between the plane of reference and plane for which the displacement x is being measured.

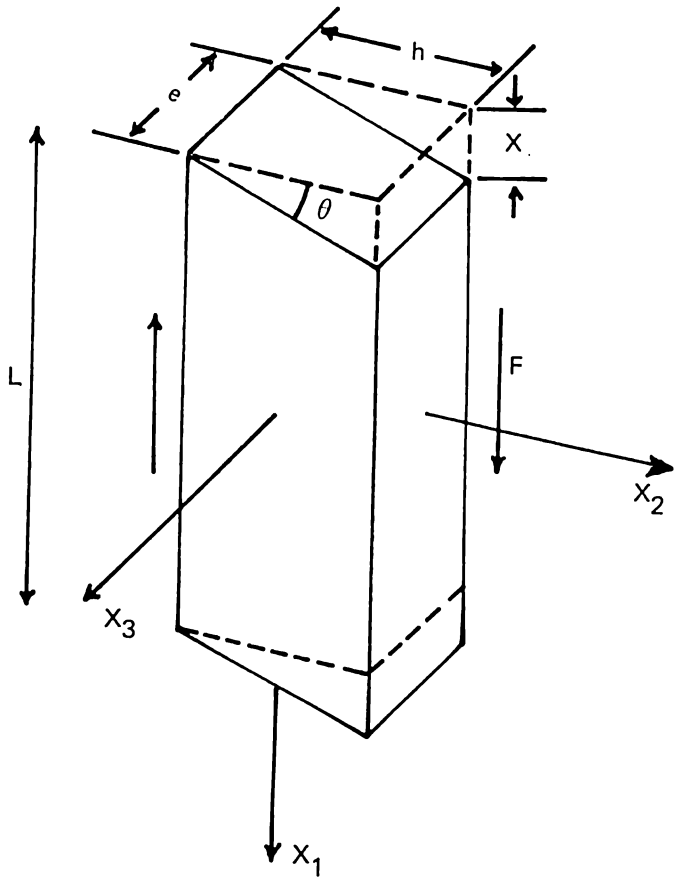

Figure 3: Geometry of plane simple shear

– Stress $= F / L.e$

– Strain $\gamma = x / h$

In an orthogonal system of reference $Ox_1 x_2 x_3$, the equations of the displacement field for any point in the deformed solid can be written as:

$$x_1' = x_1 + \gamma(t)\, x_2$$

$$x_2' = x_2$$

$$x_3' = x_3$$

where x_1', x_2', x_3' are the coordinates of the point after deformation and x_1, x_2, x_3 are the coordinates before deformation. γ (t) is the shear strain of the material at time t.

The shear testing apparatus (Figure 4) was designed in order to transform the coaxial force system delivered by a standard tensile testing machine into a system of parallel shearing forces.

The principal elements of the apparatus are: (Boni, 1981)

(1) the longitudinal slider (LS) which produces the simple shearing action on the specimen (S) by its offset sliding movement;

(2) the holding frame (HF) which contains the guide rails and the transversal stress and displacement gauges;

(3) the transverse slider (TS) which allows movement in a direction perpendicular to the shear axis. The sheared width h can be kept constant during a test by holding this slider firmly in place. For different specimen dimensions, the transverse slider can be moved to change the sheared width h.

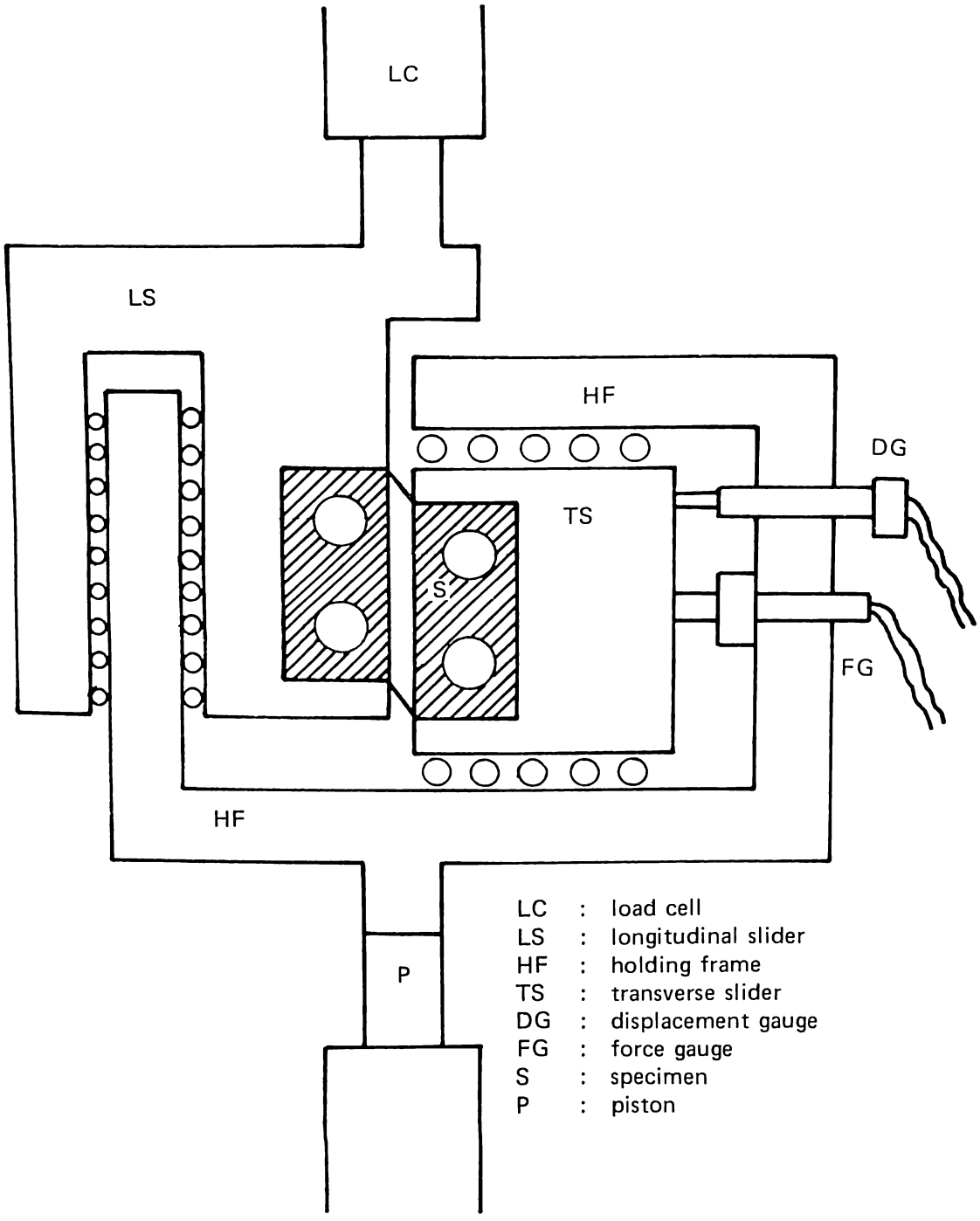

Figure 4: Schema of the simple shear testing apparatus

During all the tests in this study the transverse slider was held firmly in place such that the sheared width remained unchanged during the deformation of the specimen. The shear testing apparatus was used with an electronically-controlled hydraulically-powered universal testing machine (MTS 810). The longitudinal slider was connected to the load cell and the fixed crosshead of the testing machine while the holding frame end was attached to the piston.

The test data was recorded in the form of shear stress (τ) vs shear strain (γ) curves with all the tests being done at a constant strain rate ($\dot{\gamma}$). The shear stress τ is equal to the ratio F/S with F being the force applied as measured by the load cell (in Newtons, N) and S being the cross sectional area of the specimen (in mm^2) which is parallel to the shear plane. The area S

is then equal to the product L·e, with L being the length and e being the thickness of the specimen's calibrated part. Shear stress is expressed in megapascals, MPa (1 MPa = 1 N/mm^2).

The shear strain γ is measured with a modified electro-mechanical analog extensometer. This is described in detail in a later section of this article.

A Sefram x-y plotter (Model T2Y) directly linked to the testing machine was used to record the shear stress vs shear strain curve.

Test Specimens

The form and dimensions of the shear test specimens were determined during the conception and development of the shear testing apparatus. Three factors turned out to be important: (Boni, 1981; G'sell et.al., 1983).

(1) reduction of the end effects and the normal forces which appear during the test due to grip constraints;
(2) elimination of the risk of buckling of the specimen's calibrated part during straining; and
(3) utilization of the range of forces available from the testing machine (up to 50 kN for the MTS).

End effects are due to the free surfaces at the specimen ends and the deviation from simple shear conditions towards the extremities of the specimen. Normal forces are generated by the couple which results from the simple shear force configuration (Boni, 1981). Buckling takes place if the specimen is too thin. This phenomenon has been observed in the shear testing of polymer films (Robertson and Joynson, 1966 and 1968; Brown et. al., 1968; Boni, 1981; Boni et. al., 1982). The specimen cross section must also be chosen such that the force necessary to carry the test to completion can be supplied by the testing machine. A detailed discussion of these factors and the derived working equations are given in previous publications (Boni, 1981; G'sell et. al., 1983).

A standard specimen (see Figure 5) is square-shaped, usually cut out of an extruded or injection-molded polymer plate, and contains two square grooves machined on each side of the plate and opposite each other. The area with the reduced thickness forms the calibrated

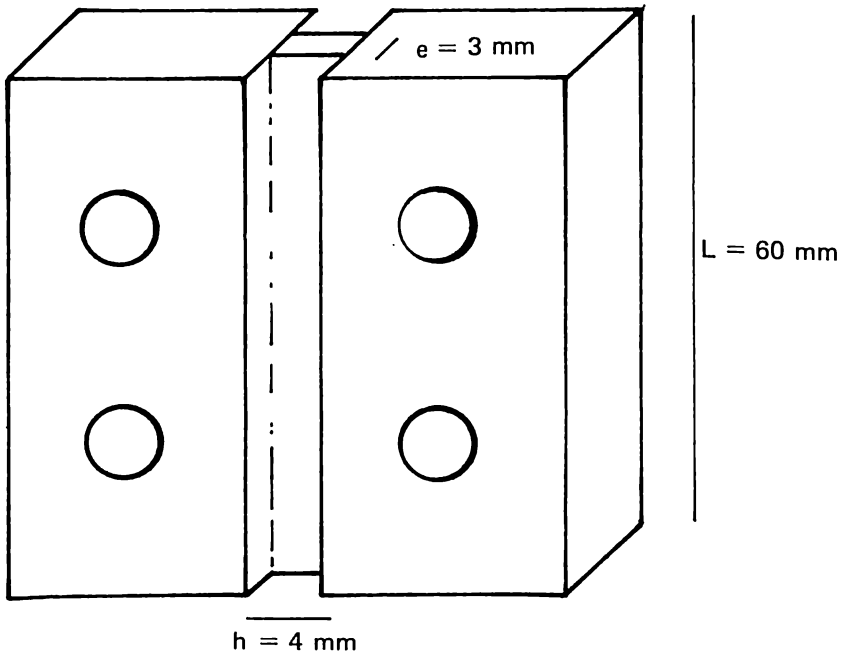

Figure 5: Form and dimensions of a shear test specimen

part on which the test is actually carried out. On either side of the calibrated part, the thicker portions of the specimen serve for gripping the specimen in the shear test apparatus. Holes are drilled in precise locations in these "heads" for the accurate positioning and the adequate gripping of the specimen in the testing apparatus. The specimen is mounted with its long dimension (length) of the calibrated part parallel to the shear direction.

The calibrated part of a typical shear specimen has a length L = 60 mm, a thickness e = 3 mm and a width h = 4 mm. The specimens were made from square blanks with a horizontal shaper. To insure precision in the machining, a specimen holder tailored to the specimen shape was used. This holder is described elsewhere (Boni, 1981).

Before each test, the specimen dimensions are determined with a caliper capable of measuring 0.01 mm. The specimens were then chosen such that the dimensions varied only within a 5 percent range: L = 60 ± 1mm; h = 4.00 ± 0.05mm; and e = 2.95 ±0.15mm.

Shear Strain Measurement

The shear strain γ (= x/h) is measured with an electronic analog extensometer (MTS 632–12) modified according to the schema shown in Figure 6. In place of blades, needles are attached to the extensometer arms. The needles are horizontally separated by a distance h, which corresponds to the sheared width. This distance is measured with a movable stage measuring microscope before the test. The relative displacement x in the specimen is measured by the movement of the lower extensometer arm. By calibrating the x-y plotter, a direct recording of the shear strain value can be made (γ = x/h; x = extensometer signal). This means of measuring the shear strain was designed and first used on polycarbonate due to its higher viscoelastic response as compared to polyethylene (Gopez, 1983).

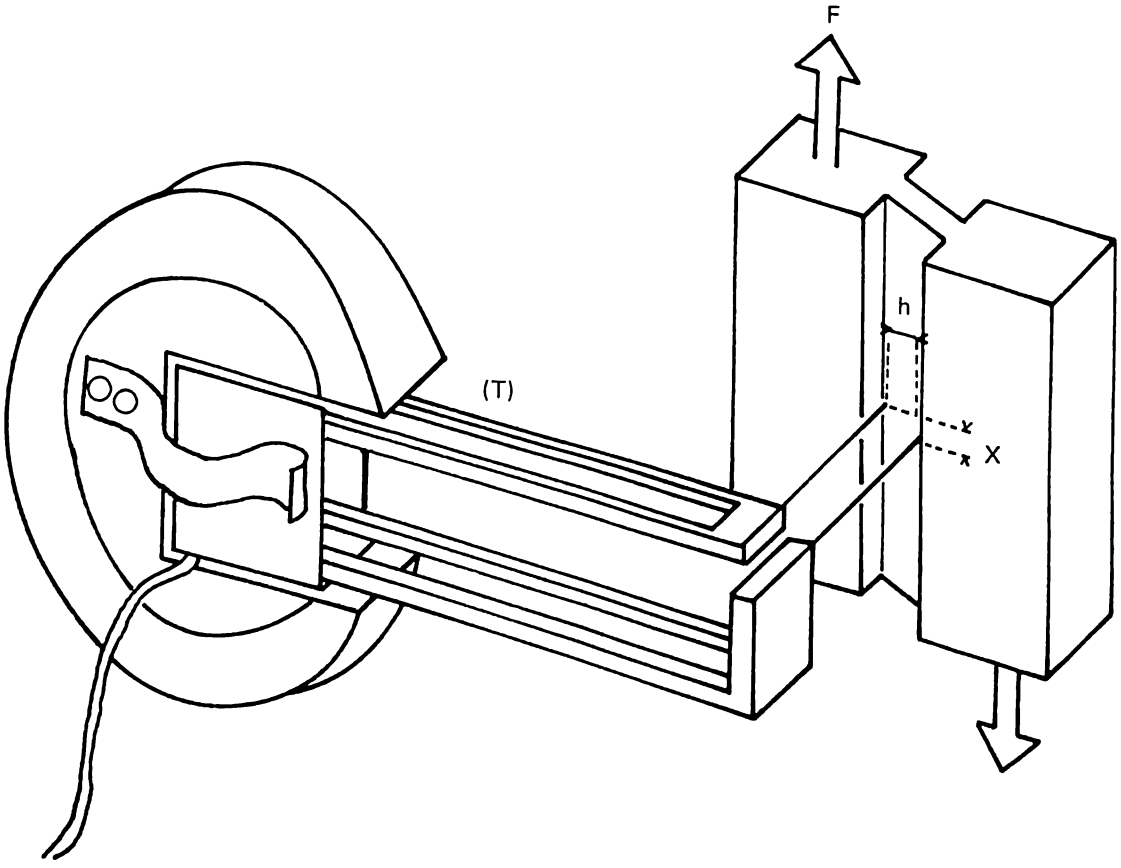

Figure 6: Shear strain transducer.

Cyclic and Reverse Shear Tests

The cyclic shear test is conducted by first deforming the specimen past the yield point, then reversing the shear direction until the specimen is brought back to a state of zero strain. The test is then continued by shearing again in the original shear direction.

Reverse shear testing involves a predeformation cycle as in the cyclic shear test but the test is continued by shearing in the direction opposite to the original shear direction.

Low-frequency Plastic Fatique Test

This test is carried out by shearing the specimen in alternate directions up to fixed values of shear strain in the plastic range. This was carried out over a few cycles at ambient temperature and at a constant strain rate of $\dot{\gamma} = 3\ 10^{-3}\ s^{-1}$. This gave an effective test frequency of about one cycle every 10 minutes.

Environmental Chamber

An environmental chamber specially designed and adapted to the shear testing apparatus enabled tests to be carried out at temperatures ranging from −100°C to 300°C. Cooling to −40°C is done through a freon-based refrigeration unit. For lower temperatures the chamber is equipped with a second circuit which has a low-pressure liquid nitrogen heat exchanger.

Thermostats linked to two internal thermocouples regulate the chamber temperature. The big thermal mass of the shear testing apparatus makes attainment of operating temperatures a rather long procedure (12 to 16 hours) even if the circulating air rapidly reaches the required temperature (less than one hour). This thermal mass is an impediment at the start of tests but once the temperature is reached, the same thermal mass prevents excessive fluctuation of temperature. Usual fluctuations never exceed ± 65°C after stabilization (Boni, 1981).

Characterization Techniques

To gain information on the plastic deformation process, a number of specimens were deformed to different values of plastic shear strain. Samples containing the sheared part were then cut out of the specimens. The samples were polished to remove the machining scratches and to render them transparent. Photographs of the polished samples were taken with an Olympus OM2 equipped with a macro objective (Olympus Zuiko MC 50 mm F3.5). These observations were carried out only for specimens deformed at ambient temperature and at a reference strain rate $\dot{\gamma} = 3\ 10^{-3}\ s^{-1}$.

Polishing of samples was done by first using abrasive paper (1200P Grit) to remove the machining marks and then by using diamond paste with progressively smaller particles (6 m to 0.25 m). A disk polisher (Struers) with interchangeable lubricated horizontal disks was used for this purpose.

RESULTS

Mechanical Behavior of Polycarbonate in Simple Shear

The Shear Stress τ vs Shear Strain γ Curve

A typical shear stress τ −shear strain γ curve for polycarbonate is shown in Figure 7. This curve was obtained at ambient temperature (23 ± 1°C) and at a constant strain rate ($\dot{\gamma}$) of $3\ 10^{-3}\ s^{-1}$. The curve can be divided into five stages.

Stage I corresponds to the almost linear portion of the curve with an initial slope of about 420 MPa. At around $\gamma = 0.1$, the slope of the curve diminishes gradually causing the curve to be concave downwards. During this short stage which goes only up to $\gamma = 0.2$, the

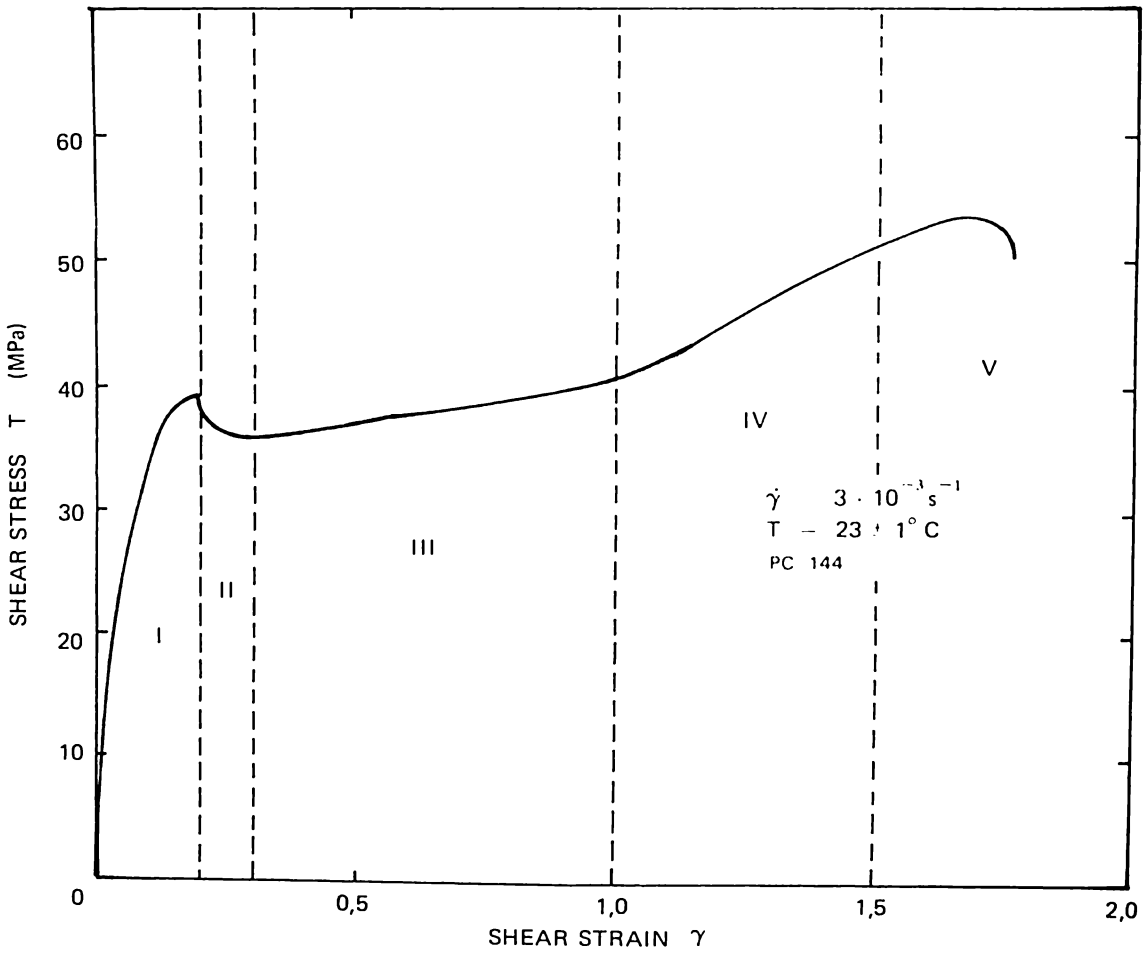

Figure 7: Shear stress vs shear strain diagram of polycarbonate

deformation is recoverable within a time span equal to the loading time when the load on the specimen is removed. If unloading is done at shear strains less than five percent, the behavior of the material is almost entirely elastic. If the unloading is done at higher strains, a viscoelastic response causes some residual deformation but this is entirely recovered in less than one hour ($t < 2000$ s) after unloading.

The shear strain transducer allows a good determination of the material's shear modulus G. The value obtained, 420 MPa, is however smaller than the dynamic shear modulus measured at 1Hz and at 23°C by Heijboer (1977) which is 820 MPa for polycarbonate. Comparison with calculated values based on the Young's modulus (E) as given by the manufacturer also shows a discrepancy. Using the expression $G = E/2(1 + \nu)$ where ν is Poisson's coefficient gives $G = 790$ MPa for $\nu = 0.4$ which is a generally accepted value for polymers (see for example S. Turner, 1974). A finer approximation can be had by using $\nu = 0.31$, a value measured by Whitney and Andrews (1967) using dilatometry. This gives $G = 840$ MPa. All three values cited fall in a range of six percent. The difference between these values and that obtained by the shear test may be due to that the simple shear test gives a secant modulus while dynamic testing measures a tangent modulus at very small strains. The simple shear test is also carried out at a much slower strain rate than dynamic measurements.

Stage II is characterized by a stress drop even as the strain increases from 0.20 to $\gamma = 0.30$. The maximum shear stress (τ_{max}) is equal to 38.5 MPa (± 0.5) while the stress at the end of the stage is 35.5 (± 0.5) MPa. Unloading tests indicate that the shear strain at this stage is no longer totally recoverable. A residual strain persists for a long time at room temperature. This residual strain will be referred to as "plastic strain" throughout the rest of this article.

Stage III is a linear part of the curve with a slope of only 7 MPa. This stage, which is the longest, stretches from $\gamma = 0.3$ to $\gamma = 1.0$. It is to be noted that at the end of this stage the shear stress (τ) is back to the same value of the maximum shear stress (τ_{max}) before the stress drop.

Stage IV is another linear portion with a steeper slope of about 21 MPa. This stage goes from $\gamma = 1.0$ to $\gamma = 1.5$. Towards the end of this stage, the slope starts to diminish.

Stage V is the rupture stage. The slope of the curve decreases progressively and finally becomes negative at $\gamma = 1.7$. A sudden stress drop indicates specimen rupture. This usually takes place at around $\gamma = 1.8$.

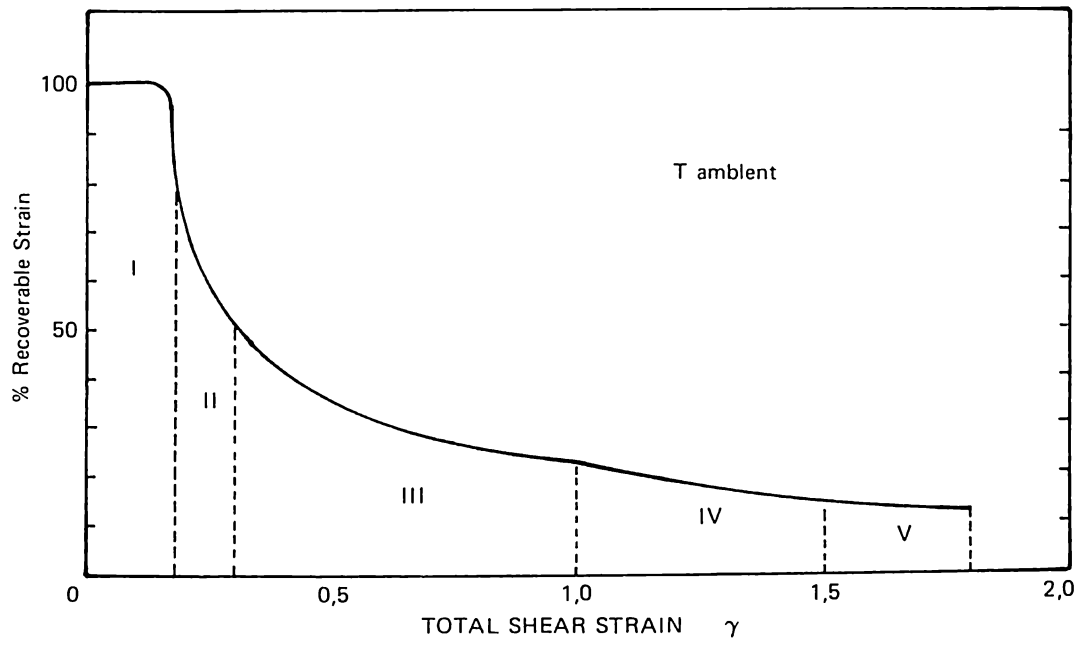

Figure 8: Percentage of recoverable strain as a function of total strain

Figure 8 gives the results obtained from unloading tests carried out at different points on the shear stress-shear strain curve. The results show that all the deformation is recoverable during Stage I and that plastic deformation becomes apparent in Stage II. The fraction of recoverable strain decreases rapidly during Stages II and III. At rupture the recoverable strain is only 11 percent of the total strain.

INFLUENCE OF STRAIN RATE AND TEMPERATURE

Shear tests were done at four different strain rates ($\dot{\gamma}$) ranging from $3\ 10^{-5}\ s^{-1}$ to $3\ 10^{-2}\ s^{-1}$ at three different temperatures ($T = -24°C$, $T = 23°C$, $T = 120°C$). Figure 9 shows the curves obtained. The maximum shear stress (τ_{max}) increases with the strain rate (from 34 to 40 MPa at $T = 23°C$). For a given temperature, the curves obtained at different strain rates are parallel to each other starting from the stress drop (Stage II). Only the curves obtained at $\dot{\gamma} = 3\ 10^{-2}\ s^{-1}$ approach or intersect the other curves. This is attributed to the self-heating effect which develops during very rapid straining of polymers. The same phenomenon has already been observed in tensile testing (Cornes et. al., 1977) and in the simple shear testing of high density polyethylene at $\dot{\gamma} = 1\ 10^{-1}\ s^{-1}$ (Boni, 1981; G' sell et. al., 1983). Self-heating has a softening effect on the polymer and would therefore account for the appearance of the curves obtained at the most rapid strain rate used. In the present case, self-heating is less evident at 120°C and its effects are felt only after the start of plastic deformation (after Stage II). It would seem then that it is the work that produces plastic deformation which is responsible for the self-heating effects.

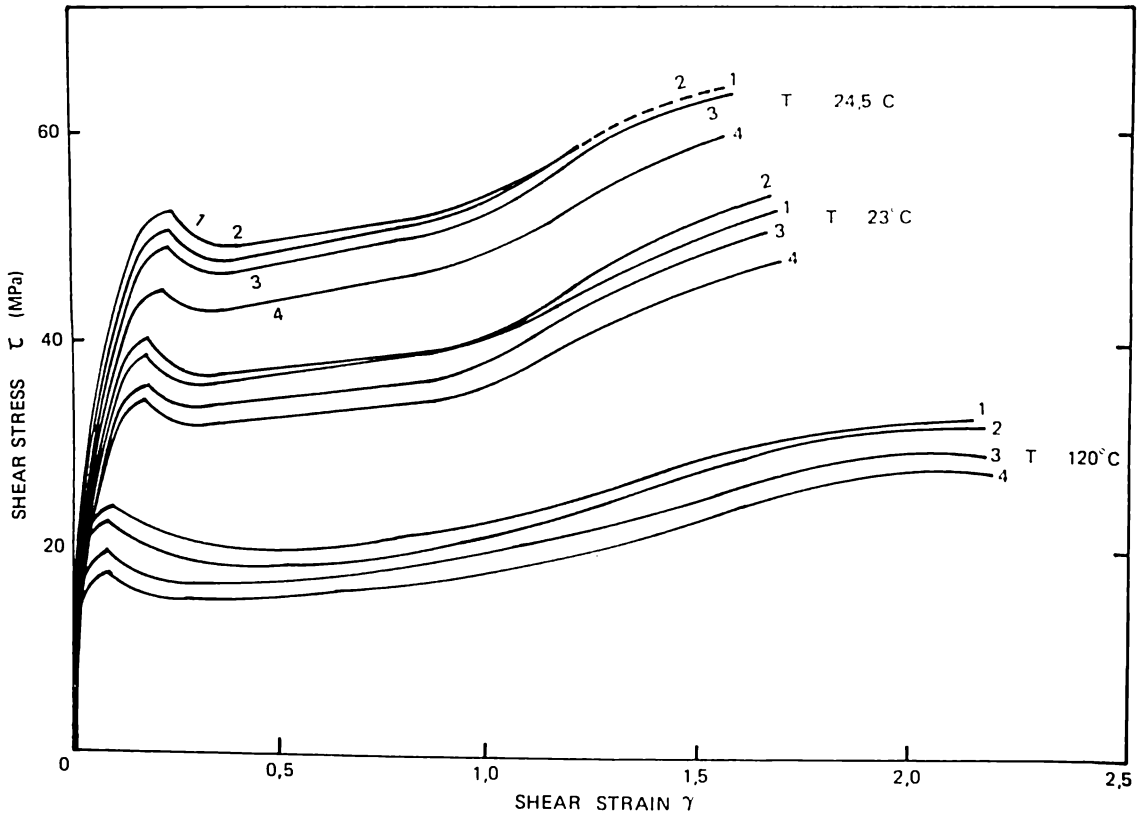

$T = -24,5°C$

N° 1	$\dot{\gamma} = 3.10^{-2}\ s^{-2}$	PC47 c
N° 2	$\dot{\gamma} = 3.10^{-3}\ s^{-1}$	PC172
N° 3	$\dot{\gamma} = 3.10^{-4}\ s^{-1}$	PC25 c
N° 4	$\dot{\gamma} = 3.10^{-5}\ s^{-1}$	PC23 c

$T = 23°C$

N° 1	$\dot{\gamma} = 3.10^{-2}\ s^{-1}$	PC148
N° 2	$\dot{\gamma} = 3.10^{-3}\ s^{-1}$	PC144
N° 3	$\dot{\gamma} = 3.10^{-4}\ s^{-1}$	PC153
N° 4	$\dot{\gamma} = 3.10^{-5}\ s^{-1}$	PC158

$T = 120°C$

N° 1	$\dot{\gamma} = 3.10^{-2}\ s^{-1}$	PC58 c
N° 2	$\dot{\gamma} = 3.10^{-3}\ s^{-1}$	PC167
N° 3	$\dot{\gamma} = 3.10^{-4}\ s^{-1}$	PC50 c
N° 4	$\dot{\gamma} = 3.10^{-5}\ s^{-1}$	PC73 c

Figure 9: Effects of strain rate on the shear response of polycarbonate

The effect of the strain rate can be better seen by looking at the $\ln \tau - \ln \dot{\gamma}$ curves shown on Figure 10. All the curves are parallel to each other, but do not pass through the data points obtained at $\dot{\gamma} = 3\ 10^{-2}\ s^{-1}$ as already mentioned. It is to be noted that the stress increases by only seven percent when the strain rate is increased by a factor of 10.

Figure 11 shows the curves obtained at temperatures ranging from −100°C to 150°C. These tests were conducted at a reference strain rate of $\dot{\gamma} = 3\ 10^{-3}\ s^{-1}$.

The initial slope (Stage I) of the curves decreases as the temperature is increased. At low temperatures (−100°C), this slope has a high value (about 600 MPa). Its value decreases slowly as the temperature is increased to 135°C. Between 135°C and 143°C, the slope decreases abruptly, from 320 to only 80 MPa, or by a factor of 4. At 150°C, the slope is even less, only 30 MPa.

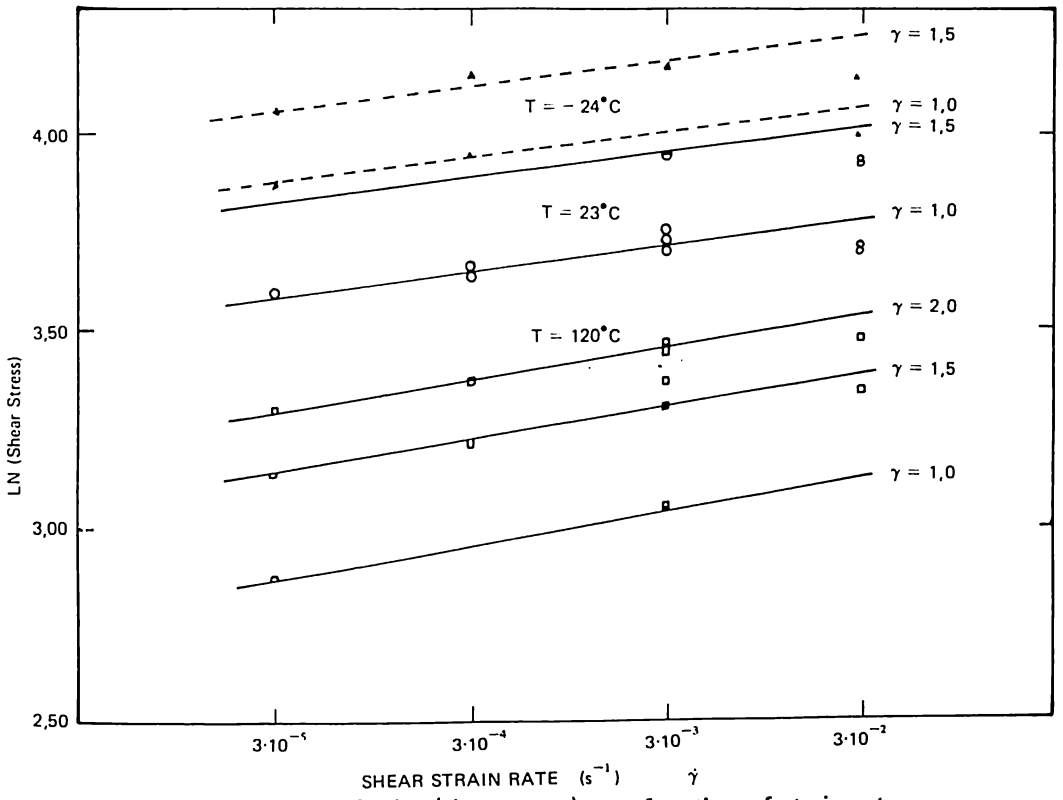

Figure 10: Ln (shear stress) as a function of strain rate

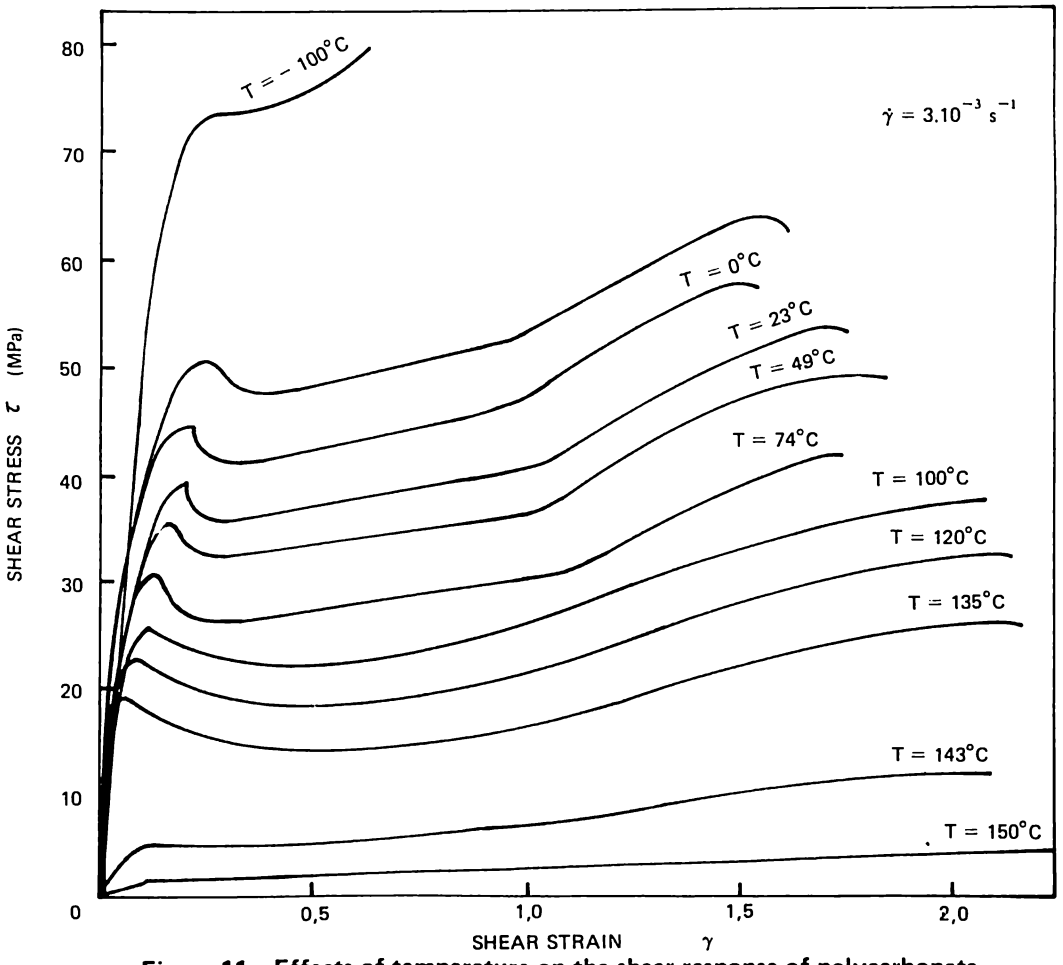

Figure 11: Effects of temperature on the shear response of polycarbonate

T	PC N°
− 100 °C	78 (corrige)
− 24,5 °C	172
0	170
23	144
49	31 (corrige)
74	164
100	38 (corrige)
120	167
135	168
143	161
150	01

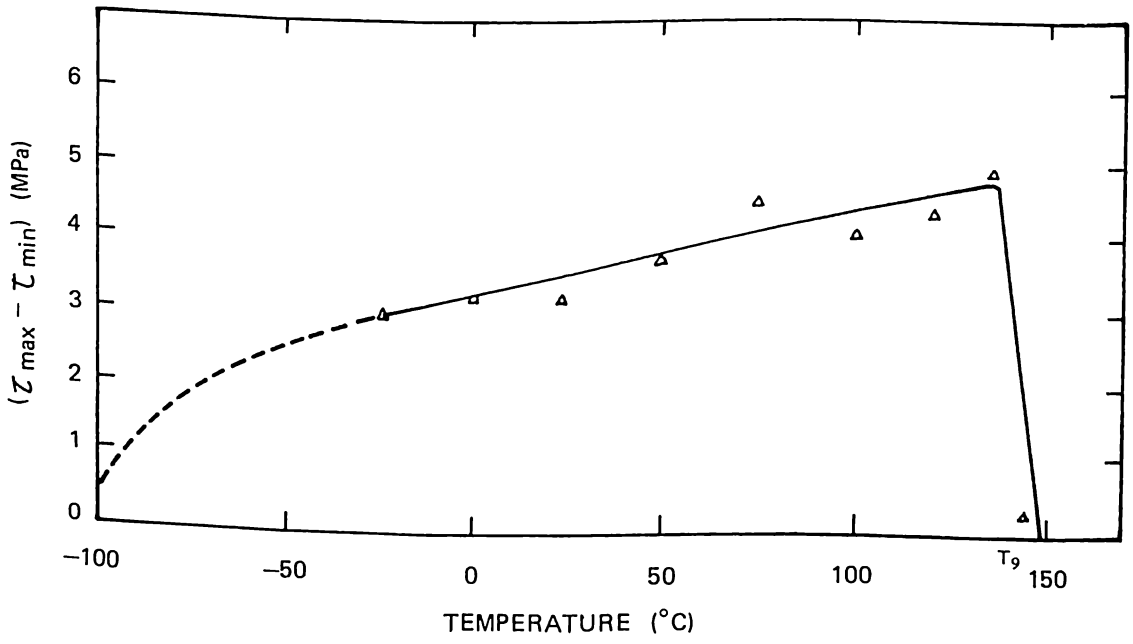

Figure 12: Variation of the stress drop amplitude as a function of temperature

The stress drop (Stage II) is no longer apparent at low temperatures (−100°C) and also at elevated temperatures (from 143°C). The amplitude of the stress drop seems to increase with the temperature and reaches its maximum value at 135°C, just before the glass transition takes place (Figure 12).

The appearance of the curves at large strains varies widely with the testing temperature. Using the curve obtained at 23°C as reference, it can be said that at low temperatures there is a gradual diminution of the length of Stage III and an increase in the slope of Stage IV. At the same time, the strain at rupture decreases with the temperature. This change in response is such that at −100°C, the material exhibits an elastic-plastic behavior with a very high strain hardening coefficient and a rupture strain of only 0.75. On the other hand, when the temperature is increased, the slope of Stage IV decreases gradually even as the stress drop extends over a wider range of strain. Eventually the two stages (III and IV) merge and become indistinguishable. At around 150°C the material exhibits a behavior typical of rubbery solids (elastomers).

The variation of the shear stress with temperature at the elastic limit and for fixed values of shear strain is given by the curves in Figure 13. These curves show a two-stage linear variation of stress with temperature up to 130°C where there is a sudden non linear decreas

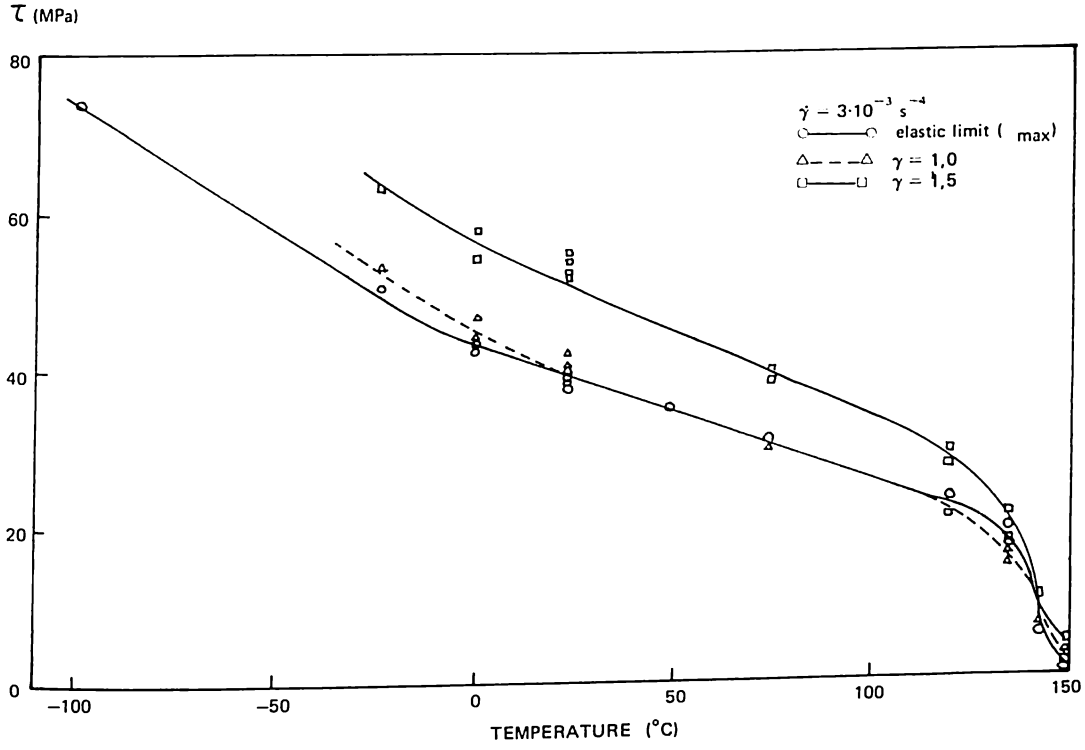

Figure 13: Shear stress as a function of temperature

in the stress value. Maximum softening is evident at about 143°C, a temperature which corresponds well with the glass transition temperature, T_g = 145°C measured by Heijboer (1977) by dynamic damping.

THE NORMAL STRESS DEVELOPED DURING SHEAR TESTING

As already stated previously, a normal stress (σ_{22}) is produced in the material during a shear test. Since the transverse slider is held in place during a test, the sheared width h remains constant and the resulting normal stress is measured as a reaction of the material against the transverse slider. This normal stress is parallel to the Ox_2 axis in Figure 3.

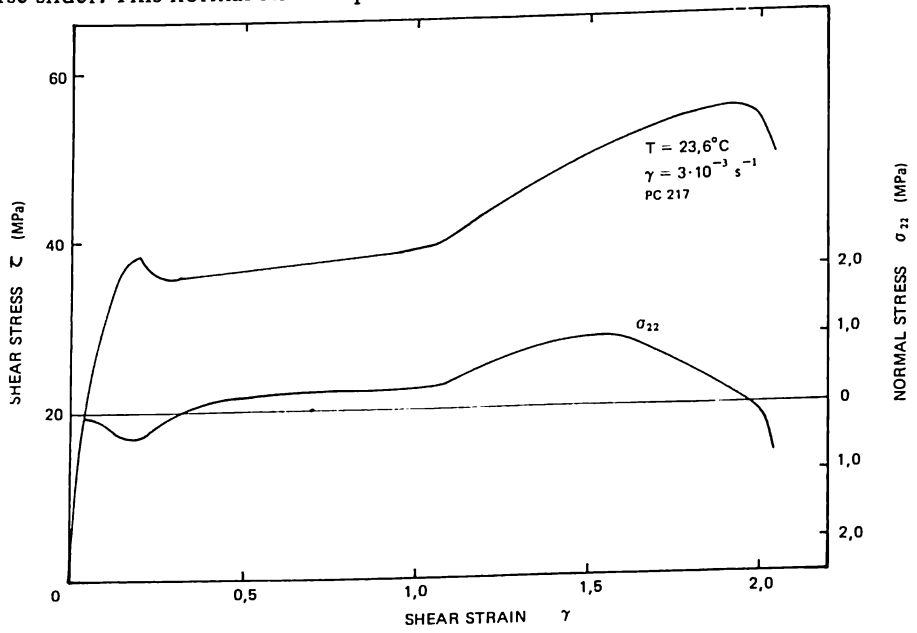

Figure 14: Normal stress (σ_{22}) vs shear strain (γ)

The lower curve of Figure 14 shows the evolution of the normal stress during a shear test at ambient temperature (23 ± 1°C) and a constant shear strain rate of 3 10^{-3} s^{-1}. The stress-strain curve is also shown in the figure to serve as a reference.

During the initial deformation stage, a compressive normal stress is registered. It increases in amplitude and attains an extremum of −0.5 MPa just before the stress drop. During Stage II the amplitude of the normal stress decreases until it changes in sign at the start of Stage III. A tensile normal stress is thus recorded during plastic deformation. This stress increases slowly in amplitude during Stage III (slope = 0.3 MPa) until it reaches a value of $\sigma_{22} = 0.30$ MPa at $\gamma = 1.0$. The curve changes its slope at the beginning of Stage IV (slope = 0.8 MPa) and the normal stress continues to increase until the middle of this stage. The maximum value of the normal stress is 1.0 MPa. Towards the end of the test the normal stress starts decreasing.

The evolution of the normal stress in the case of polycarbonate is markedly different from that observed for polyethylene (Boni, 1981; G'sell et. al., 1983). For the latter, the normal stress was compressive in nature throughout the whole test.

A simple model based on the rotation of the principal axes of the stress tensor was developed by Boni and G'sell to explain the development of a normal compressive stress in polyethylene. According to this model, the stress σ_{22} is a compressive stress whose value should theoretically follow the relation $\sigma_{22} = -0.5\,\tau \cdot \gamma_{el}$ where γ_{el} is the elastic shear strain component. In the case of polyethylene, this model agrees relatively well with experimental data.

For the present case, the normal stress σ_{22} measured at the beginning of the test is also a compressive stress. This is in agreement with the model developed for polyethylene. The comparison between observed and theoretical values, however, leaves something to be desired. At the maximum shear stress (τ_{max} = 38 MPa at γ = 0.20), the relationship $\sigma_{22} = -0.5\tau \cdot \gamma_{el}$ gives $\sigma_{22} = -3.8$ MPa while the observed value is only −0.4 MPa.

A further complication is that at the start of Stage III the normal stress σ_{22} changes in sign and becomes tensile in nature; a phenomenon not predicted by the model. The effect of the rotation of the principal stress axes or the "Kelvin effect" (Atkin and Fox, 1980) on which the model is founded cannot be questioned. A probable explanation would be the existence of an antagonistic effect with counteracts the Kelvin effect and leads to the development of a tensile normal stress σ_{22}. At the present state of investigations no such mechanism capable of explaining this phenomenon has yet been proposed.

It is to be noted, however, that the recorded normal stress σ_{22} has a very low value compared to the imposed shear stress (less than two percent of the imposed stress). This indicates that the applied shear stress is mainly responsible for the results obtained during testing.

Observations of the Deformation Process: Correlations with the Shear Stress (τ) vs. Shear Strain (γ) Curve

Figure 15 shows the photographs of samples containing the calibrated part and taken from specimens deformed to different values of plastic strain. By a difference in the optical properties between the sheared and unsheared material, a shear band can be seen to form during the straining of the specimen. The formation of this band is better understood if discussed in correlation with the different stages of the shear stress (τ) vs shear strain (γ) curve.

STAGE I ELASTIC AND VISCOELASTIC DEFORMATION

The deformation during this stage has been shown to be essentially elastic and viscoelastic in nature. The deformation is uniformly distributed in the specimen and is completely recovered upon unloading. Figure 15a shows a sample deformed up to a point in Stage I and then removed after unloading. There is no trace of any plastic strain.

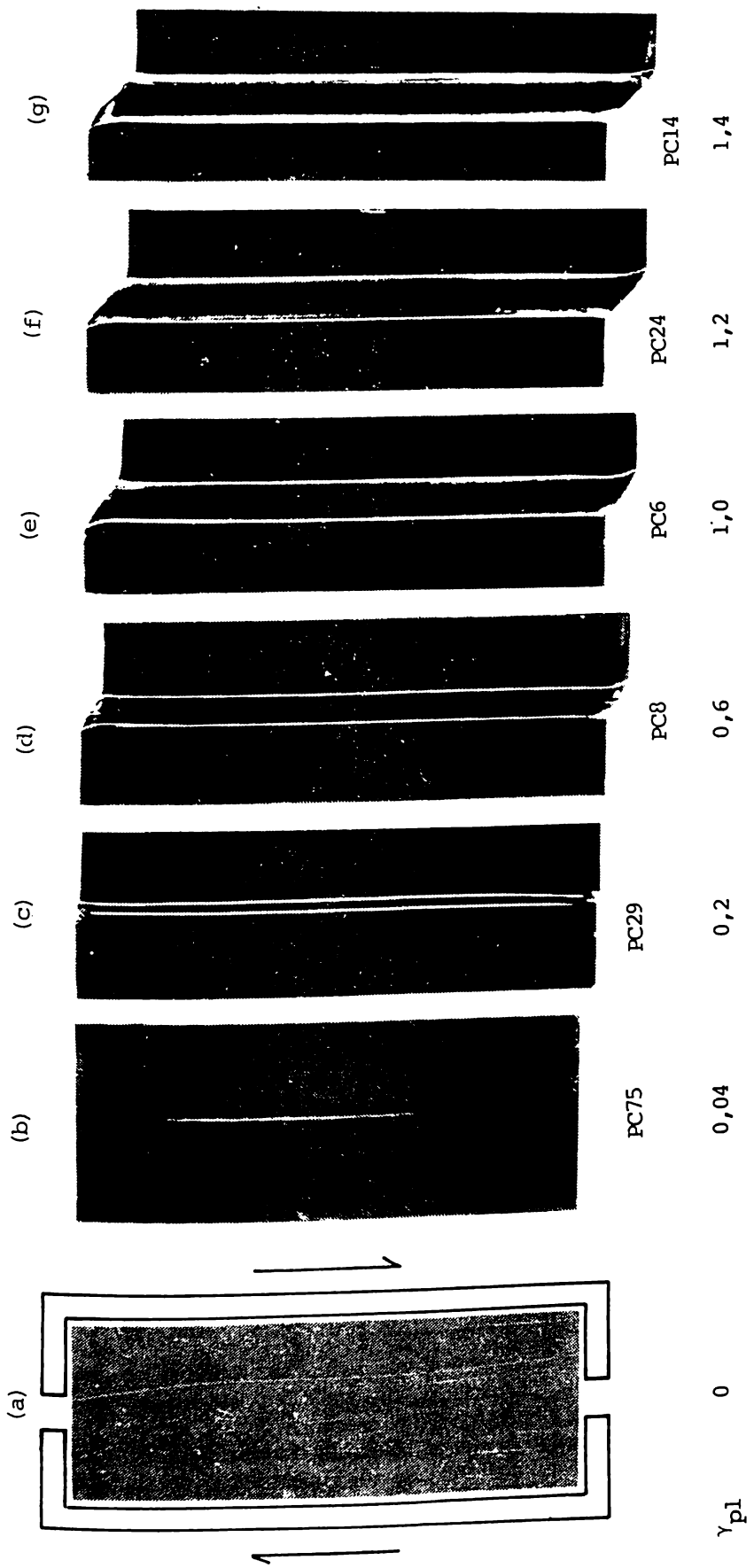

Figure 15: Shear band formation and development: samples containing the calibrated part. Straining done at ambient temperature

STAGE II FORMATION AND ELONGATION OF A SHEAR BAND

At the maximum shear stress (τ_{max}), a deformation band forms and becomes visible by a difference in its optical properties with respect to the undeformed material. This newly-formed band is visible in Figure 15b which is a picture taken of a sample deformed up to the beginning of Stage II. At this point, the band is narrow (about 0.1 mm wide) and just half as long as the specimen (25 to 33 mm). Closer investigation through the use of surface markers showed that the band is composed of plastically sheared material while outside the band only elastic and viscoelastic deformation takes place (Gopez, 1983).

During the stress drop the shear band elongates and at the end of Stage II, the band is already as long as the specimen (Figure 15c).

STAGE III WIDENING OF THE BAND

Observations show that Stage III is essentially characterized by the widening of the shear band. This is apparent from photographs c and d of Figure 15.

The end of Stage III corresponds to the point when the band has become as wide as the specimen's sheared width h. This means that the whole calibrated part of the specimen is plastically deformed. The plastic shear strain in the band is equal to the nominal shear strain of the specimen (γ = 0.80 to 0.90).

STAGE IV HOMOGENOUS PLASTIC DEFORMATION

During Stage IV the band practically occupies the entire calibrated part of the specimen. Further increase in plastic strain takes place by a uniform increase in the plastic strain of the whole specimen.

Two parasitic phenomena affect the analysis of results in Stage IV. The first is due to an extension of the plastic zone into the specimen heads. The shear strain transducer was developed to filter out this effect in order to obtain a stress-strain curve which essentially reflects the material's intrinsic properties. White zones also appear at the shear band edges during the later part of Stage IV (see Figures 15f and g). These zones form at the specimen ends and spread towards the middle portion. No detailed study of these white zones was carried out although there are some indications that these might be crazes.

STAGE V RUPTURE STAGE

Rupture starts at the specimen ends. A small crack can be seen at the lower end of the specimen in Figure 15g. These cracks are always inclined with respect to the shear direction. A scanning electron microscope study of the fracture (Gopez, 1983) shows that fracture starts by the formation of inclined lozenge-shaped cracks on the specimen surface. These cracks then penetrate into the specimen and the material between cracks is pulled apart until complete separation takes place.

End Effects

The simple shear conditions which are well verified at the specimen center change towards the specimen ends due to the free surfaces. This end effect was first investigated in polyethylene by putting a network of points on the specimen surface before testing and observing the change in the configuration of the points during the test (Boni, 1981; G'sell et. al. 1983). A similar test on polycarbonate (see Figure 16) indicates that the end effects are essentially identical in nature regardless of the material deformed. Manifestations of the end effect can be described as follows:

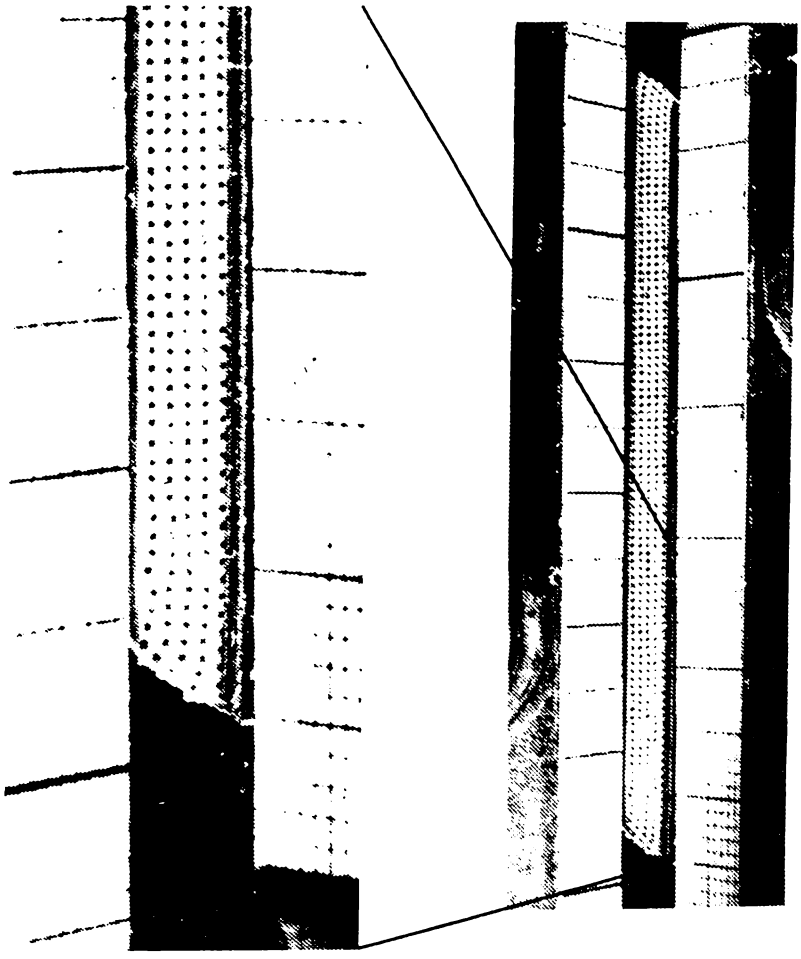

Figure 16: Network of points showing end effects during the shear testing of polycarbonate, = 1.0 (Scale: distance between points = 1.0 mm). (PC 57)

(1) The rows of points which were initially parallel to specimen length curve towards the reentrant corner of the specimen end; and,

(2) The free surface of the specimen end becomes a curved convex surface ("bulging out" of the material).

Both of these manifestations are clearly visible in Figure 15.

A computer model of the shear deformation of a material obeying a Mooney-Rivlin type law confirms the nature of the observed end effects (G'sell et. al., 1983; Gopez, 1983).

From both the experimental observations and the results of the mathematical modelling, it was shown that the end effects are felt only in an area whose length is approximately equal to the specimen width, an observation which is in agreement with Saint Venant's principle (1856).

Since the specimen width h is very much smaller than its length L (h/L = 4/60), the end effects can be considered to have a negligible effect on the shear stress-shear strain curves obtained with this testing method.

Cyclic Shear and Reverse Shear Test Results

CYCLIC SHEAR TEST

The cyclic deformation test was performed at ambient temperature (23 ± 1°C) at a constant strain rate ($\dot{\gamma} = 3\ 10^{-3}\ s^{-1}$). Figure 17 shows the results. The specimen is first

deformed up to the start of Stage IV such that all of its calibrated part is plastically deformed. The shear direction is then reversed and the specimen is brought to a state of zero macroscopic shear strain (curve in dots). At this point the specimen looks like an undeformed specimen without any external indication whatsoever of its previous mechanical treatment.

The specimen is then redeformed by shearing in the original direction. The curve obtained (continuous line) has a less steep initial slope (about 160 MPa) and shows a less abrupt transition between the elastic and plastic ranges. The apparent elastic limit is only $\tau_y =$ = 18 MPa. The shear strain at the elastic limit is still $\gamma = 0.20$. Beyond this point the shear stress τ varies in a linear fashion with shear strain γ. At large strains ($\gamma > 1.0$), the curve is almost identical to that of a previously undeformed specimen (dashed lines in Figure 17). There is, however, a difference of 1 MPa between the two curves, with the cyclic test having the lower values. Tests stopped just after the apparent elastic limit showed that for a cyclic test specimen the whole calibrated part was already plastically deformed as early as this point. The shear band already occupied the whole calibrated part immediately.

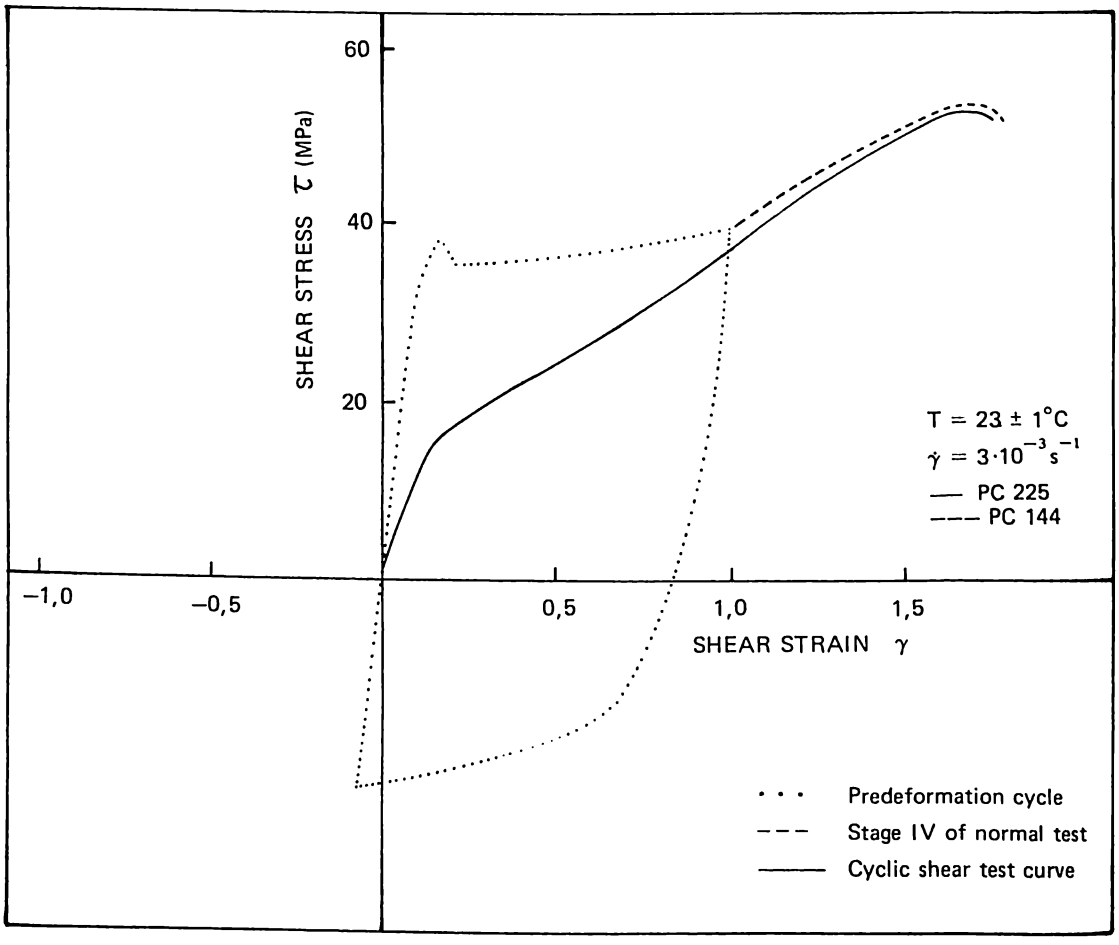

Figure 17: Cyclic shear test curve

REVERSE SHEAR TEST

In the reverse shear test, whose results are shown in Figure 18, the specimen is deformed up to Stage IV and then brought back to a state of zero strain. The test is then continued by shearing in a direction opposite to the initial shear direction. The curve obtained shows a steeper slope in the elastic range, a well-defined elastic limit, a small stress drop after the limit, and an almost linear portion at the end. Comparison with the curve of a previously undeformed specimen shows that the two curves are parallel at large strains (Stage IV for a normal test), but the reverse shear test curve has values higher by 5 MPa. A similar result was reported by Wu and Turner (1973) in the torsion testing of polycarbonate. In their experiment the reverse test curve was higher than the direct test by about 3 MPa.

As in the previous case, unloading tests showed that right after the apparent elastic limit, the reverse shear specimen was homogenously deformed.

SHEAR TEST OF A SPECIMEN ANNEALED AFTER A PLASTIC DEFORMATION CYCLE

To investigate the effects of thermal treatment, a specimen which had previously been deformed to the start of Stage IV and then brought back to zero strain was annealed for three hours at 150°C and slowly cooled before further testing. Figure 19 shows the curve obtained. It is practically identical to that of an undeformed specimen (dashed lines in Figure 19) except for a slightly higher elastic limit (τ y = 40 MPa) and a less steep slope (= 4.0 MPa) in Stage III. After annealing, the effects of the plastic deformation cycle are apparently erased and plastic deformation once more takes place with the formation and growth of a shear band.

LOW FREQUENCY FATIGUE TEST

By alternate shearing to $\gamma = 1.0$ and $\gamma = -1.0$, at a shear strain of $\dot{\gamma} = 3\ 10^{-3}\ s^{-1}$, the low frequency fatigue test was carried out at room temperature. Only a few cycles were done and cycling was not carried out until specimen failure. The results, shown on Figure 20, show a high elastic limit and stress drop only for the first cycle. The stress level then drops at the succeeding cycles and they resemble each other. There is a slight softening effect with the later cycles having stress levels lower than preceding cycles by 2 MPa.

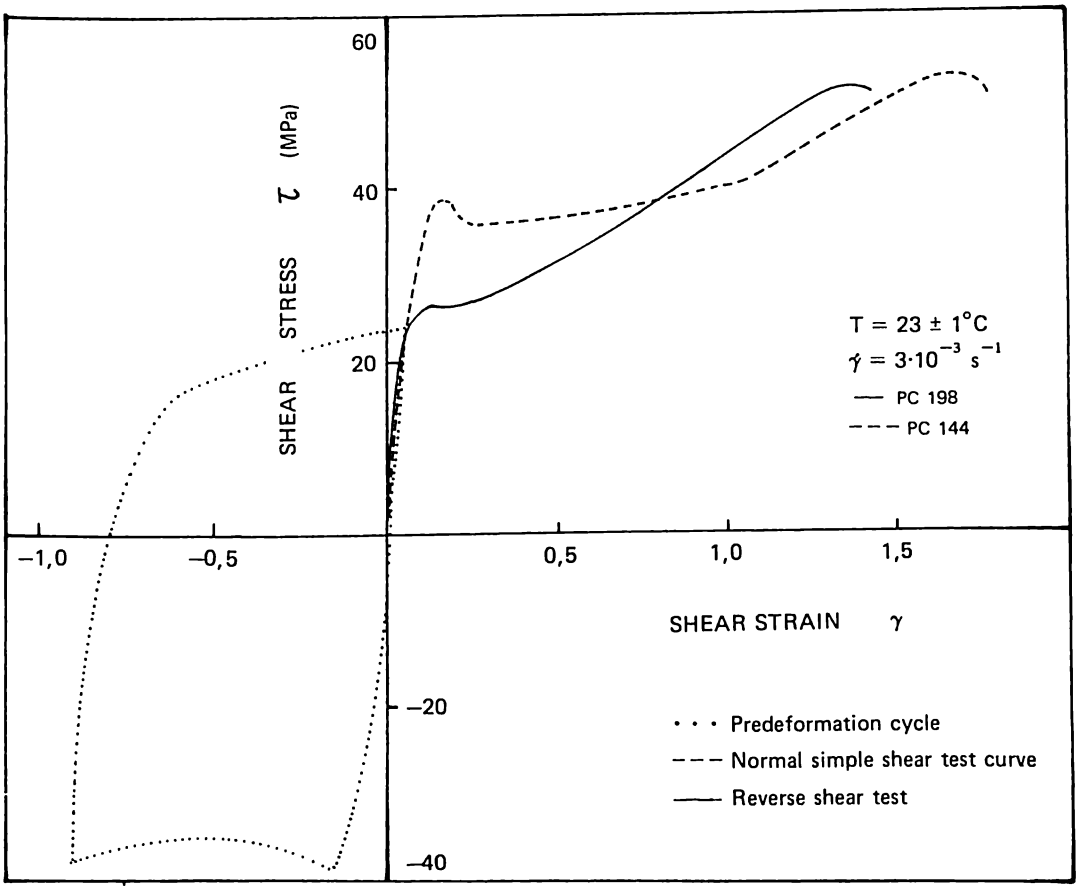

Figure 18: Reverse shear test curve.

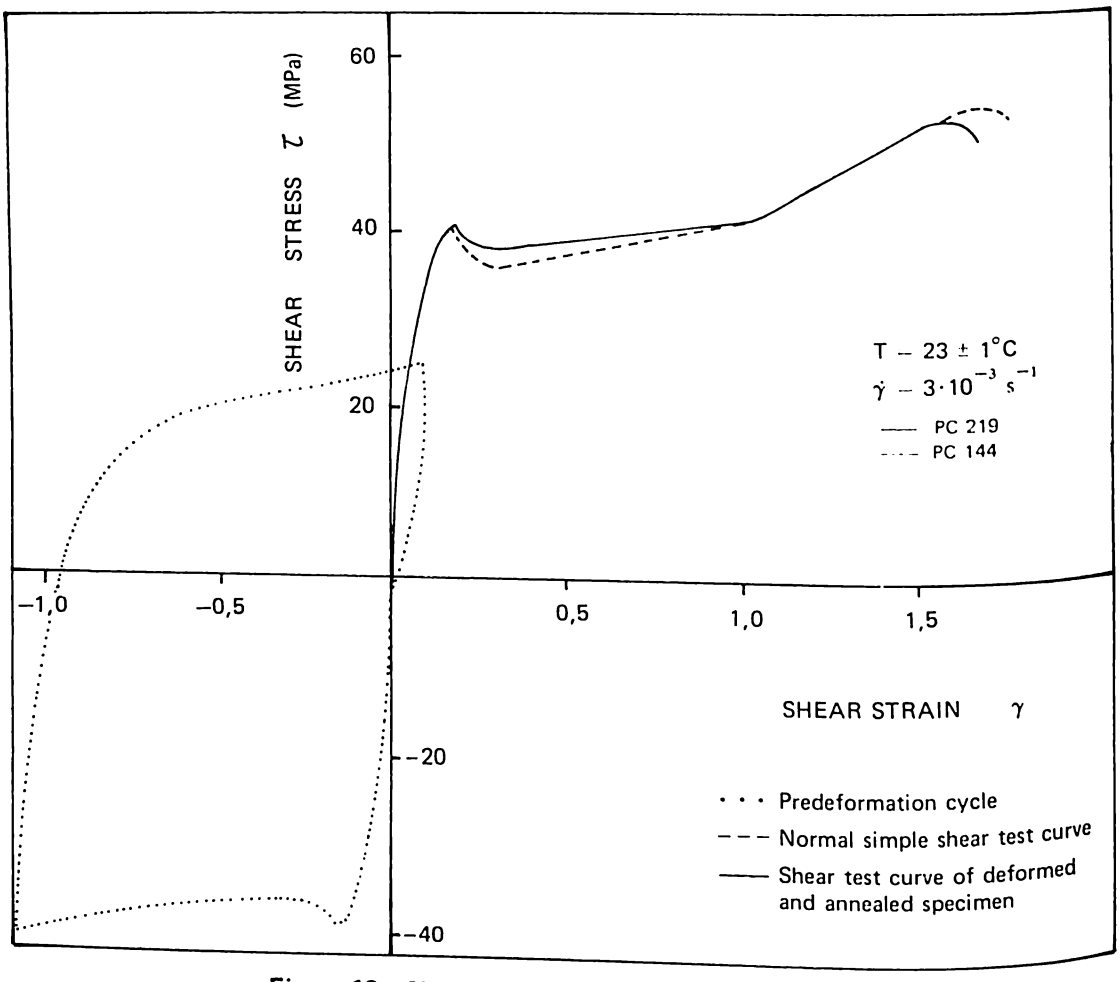

Figure 19: Shear test curve of an annealed specimen

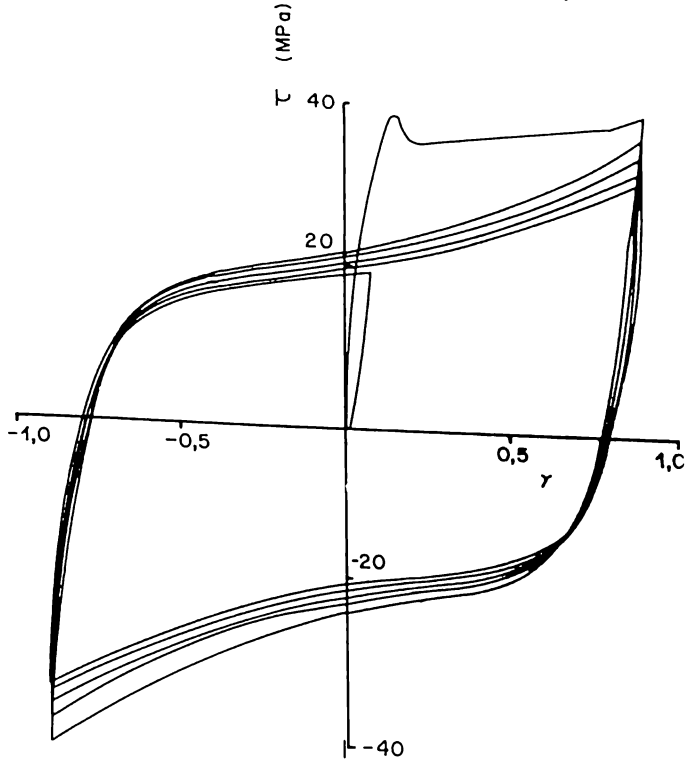

Figure 20: Low-frequency plastique fatigue test

DISCUSSION

A Constitutive Flow Equation for Polycarbonate in Simple Shear

DOMAINE OF VALIDITY OF THE FLOW EQUATION

Enough inforation is available for the formulation of a constitutive flow equation for polycarbonate in simple shear. This equation should predict the stress level for a given value of strain and vice versa in the plastic range. It is obvious that for this equation to be of any value it must be formulated for a range of strain values such that the specimen is undergoing homogenous plastic strain. This minimizes the possibilities of having extraneous phenomena such as stress concentrations or localized deformation. Stages II and III of the shear test curve are in the plastic range but they also correspond to the development and propagation of a shear band. This form of localized deformation leads to different states of strain for a single stress value, and thus renders any constitutive equation invalid. On the other hand, Stage IV corresponds to a homogeneous plastic deformation stage and may therefore be described by the flow equation. Analysis will be confined only to this stage.

It is interesting to note that during Stage IV, the stress-strain curve is essentially linear with a constant strain hardening coefficient. The strain rate has a relatively weak although significant effect while at temperatures lower than the glass transition temperature (T_g), the temperature has a strong effect on the stress level. Above Tg the polycarbonate behavior becomes rubbery. These observations are in general agreement with those for other glassy amorphous polymers tested by different methods (Bowden and Jukes, 1968; Bauwens-Crowet et. al., 1972 and 1974).

MULTIPLICATIVE LAW

Constitutive equations of flow of the multiplicative form have been used for the analysis of stress-strain curves of polymers subjected to tensile testing (G'sell and Jonas, 1979; Aly-Helal, 1982; G'sell et. al., 1983b). A simple form of this type of constitutive equation would be:

$$\tau\,(\gamma, \dot{\gamma}, T) = f_1(\gamma) \cdot f_2(\dot{\gamma}) \cdot f_3(T)$$

This expression attempts to separate the effects of the different variables from each other. By logarithmic differentiation this equation becomes.

$$d\ln\tau = \left(\frac{\partial \ln\tau}{\partial \gamma}\right)_{\dot{\gamma}, T} d\gamma + \left(\frac{\partial \ln\tau}{\partial \ln\dot{\gamma}}\right)_{\gamma, T} d\ln\dot{\gamma} + \left(\frac{\partial \ln\tau}{\partial T}\right)_{\gamma, \dot{\gamma}} dT$$

where $\left(\frac{\partial \ln\tau}{\partial \gamma}\right)_{\dot{\gamma}, T} = h$, the relative strain hardening rate;

$\left(\frac{\partial \ln\tau}{\partial \ln\dot{\gamma}}\right)_{\gamma, T} = m$, the strain rate sensitivity coefficient;

and $\left(\frac{\partial \ln\tau}{\partial T}\right)_{\gamma, \dot{\gamma}} = \theta$, the temperature sensitivity coefficient.

The Stage IV curves of $\ln\tau$ vs γ at different temperatures are shown on Figure 21. The curves are almost parallel to each other and since the slope of these curves is the parameter $h = \left(\frac{\partial \ln\tau}{\partial \gamma}\right)_{\dot{\gamma}, T}$, this parameter can be considered a constant as a first approximation approach. The actual values of h vary slightly with temperature, 0.40 h 0.57 for −24 T 135°C (Figure 22). The average value $\bar{h} = 0.50$ may therefore be used and the shear strain effects may be expressed as: $f_1(\ ) = A \exp(h)$, A being a constant.

The effect of strain rate (Figure 10) shows that $\ln\tau$ is a linear function of $\ln\dot{\gamma}$. From the curves in the figure, the strain rate sensitivity coefficient $m = \left(\frac{\partial \ln\tau}{\partial \ln\dot{\gamma}}\right)_{\gamma, T}$ may be obtained.

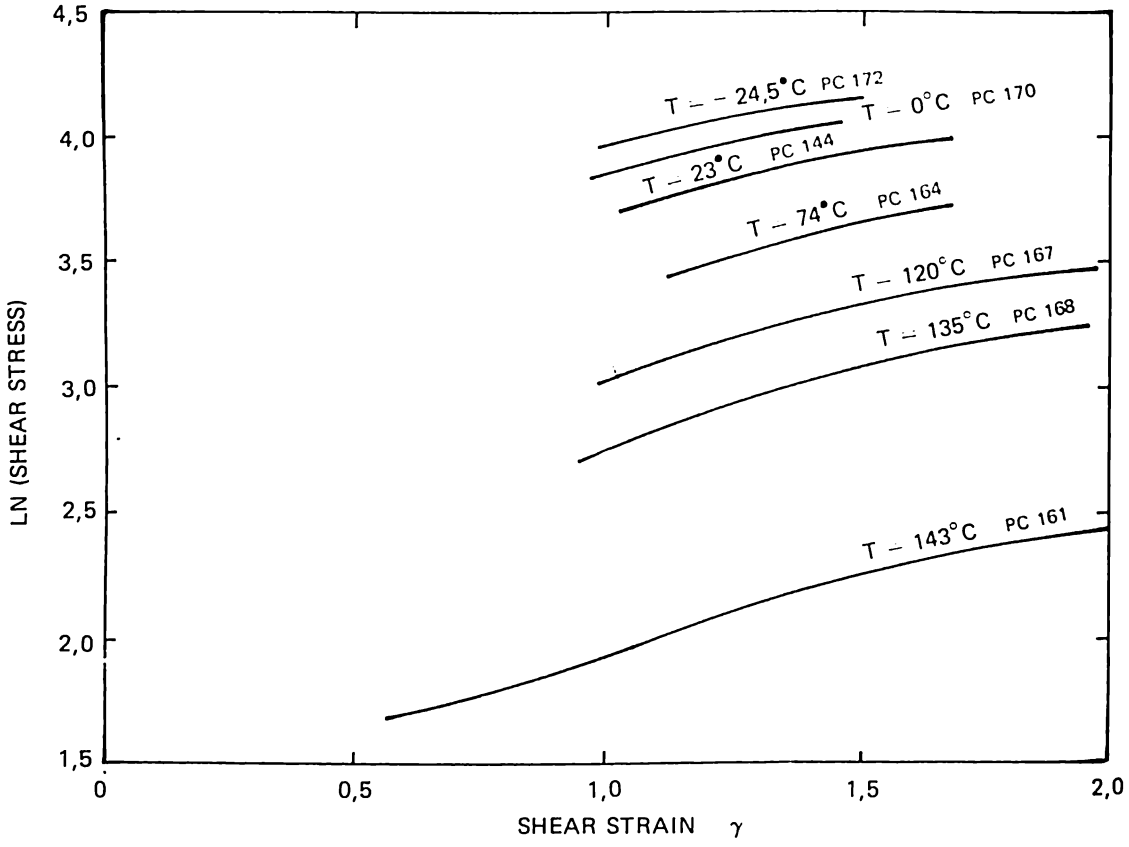

Figure 21: Ln (shear stress) vs shear strain curves at different temperatures; Stage IV only

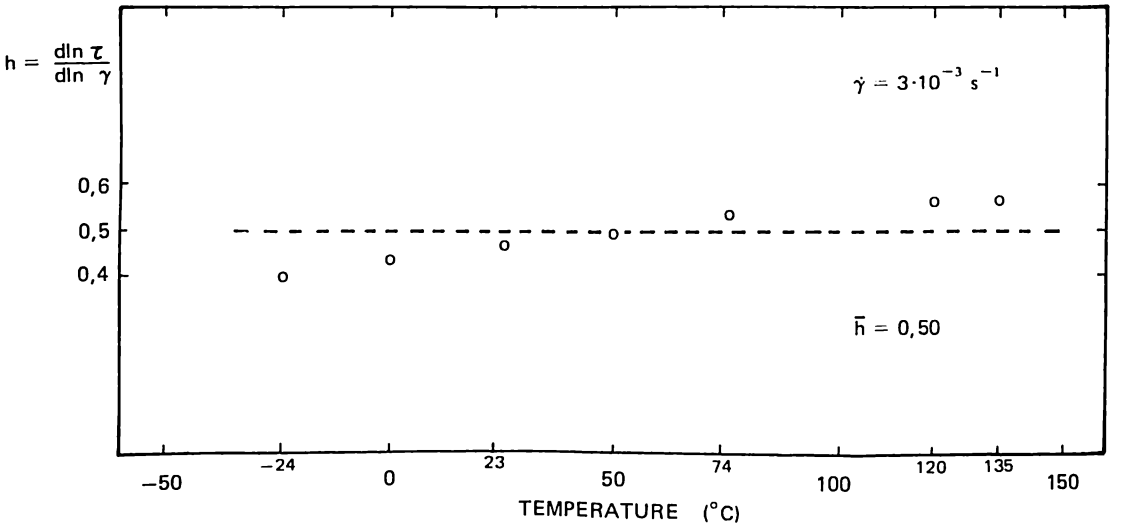

Figure 22: Relative strain hardening rate h at different temperatures

The following table gives the values of m:

T°C	γ	$m = \left(\frac{\partial \ln \tau}{\partial \ln \dot{\gamma}}\right)_{\gamma, T}$
−24	1.0	0:027
	1.5	
23	1.0	0.027
	1.5	
120	1.0	0.036
	1.5	
	2.0	

It is to be noted that m is independent of the shear strain and that it varies slightly with temperature. The strain rate effect may therefore be approximated by the relation: $f_2(\dot{\gamma}) = B\,\dot{\gamma}^m$ where B is a constant. A mean value of 0.30 may be used in this expression.

With regards to the temperature, Figure 23 shows that $\ln\tau$ is also a linear function of temperature. The slope of the curves should give the value of the temperature sensitivity coefficient $\theta = \left(\frac{\partial \ln\tau}{\partial T}\right)_{\gamma,\dot{\gamma}}$. At a reference strain rate $\dot{\gamma} = 3\ 10^{-3}\ s^{-1}$, the value of θ is constant during Stage IV, $\theta = -6.0\ 10^{-3}\ C^{-1}$. The effects of temperature may then be expressed as $f_3(T) = C\exp(\theta\, T)$ where C is a constant.

The general statement of the constitutive flow equation of polycarbonate in simple shear is:

$$\tau(\gamma, \dot{\gamma}, T) = K \exp(h\gamma) \cdot \dot{\gamma}^m \cdot \exp(\theta\, T)$$

with h = 0.50; m = 0.03; and $\theta = -6.0\ 10^{-3}\ C^{-1}$; the temperature T being expressed in degrees Centigrade. The pre-exponential factor K regroups all the constants of integration and has a value K = 32MPa.

It is to be emphasized that this is purely an empirical equation with no theoretical implications whatsoever. It is valid only in Stage IV for the range of conditions for which testing was done: $-24°C \leq T \leq 120°C$; $3\ 10^{-5}s^{-1} \leq \gamma \leq 1\ 10^{-3}s^{-1}$; and $1.0 \leq \gamma \leq 1.7$

ADDITIVE LAW

The mechanical response of materials may also be expressed in the form of an additive equation as follows:

$$\tau(\gamma, \dot{\gamma}, T) = \tau_i(\gamma, T) + \tau^*(\dot{\gamma}, T)$$

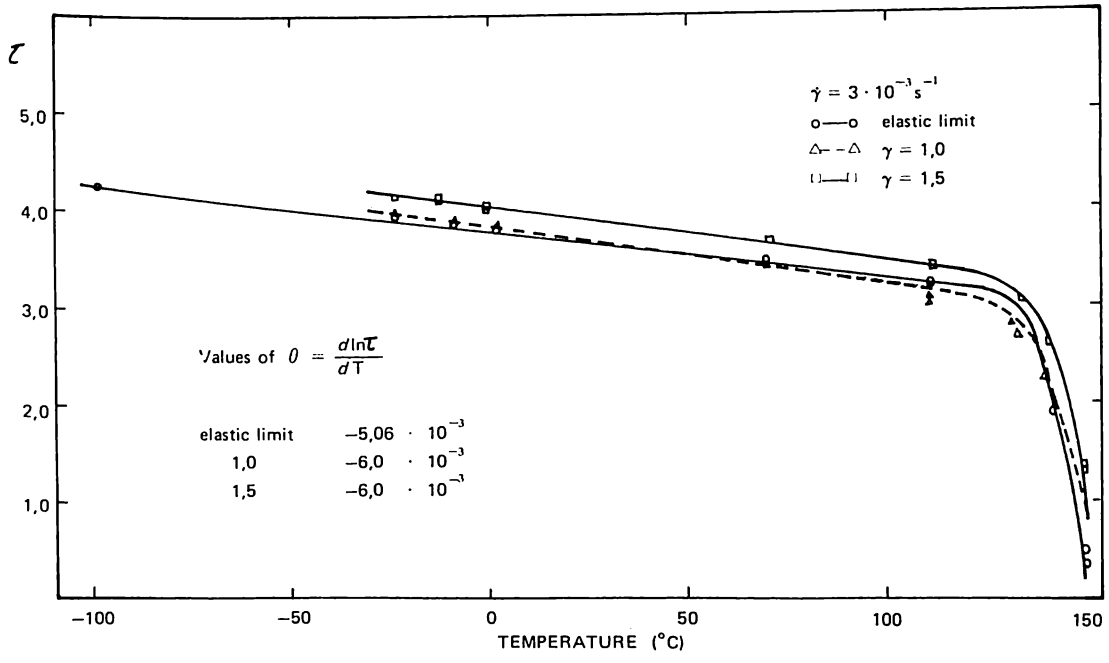

Figure 23: Ln (shear stress) vs temperature

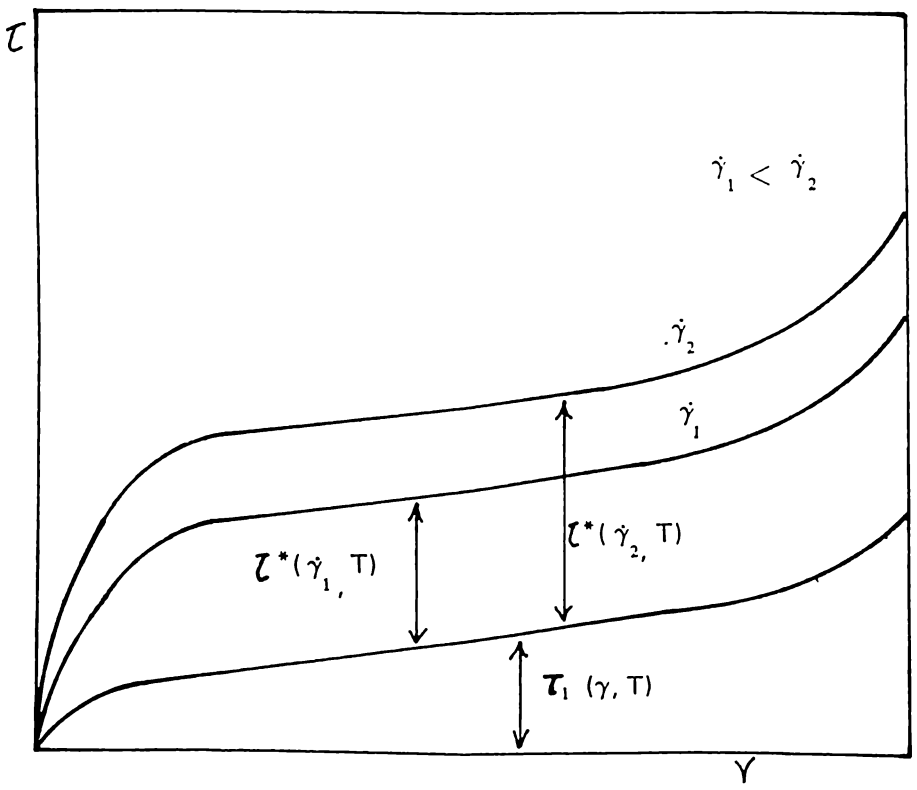

This analysis is particularly well-adapted in cases where the stress-strain curves show a simple vertical displacement as a function of strain rate. In this expression, the term τ_i, also known as the "internal stress" contains the strain effect and represents the force which tends to bring the material back to its undeformed state (Fotheringham and Cherry, 1978). The strain rate effect is contained in τ^*, the "effective stress". This term represents the stress necessary to deform the material at a higher strain rate.

Constitutive equations of the additive form have already been used for the analysis of tensile test results of polycarbonate by Bauwens-Crowet et. al. (1972 and 1974), and for other polymers (Ward, 1970; G'sell and Jonas, 1981).

A parameter which may be calculated from an additive form of the constitutive flow equation is the apparent volume of activation, v_a. Using Eyring's (1936) theory of thermal activation, the strain rate may be expressed as:

$$\dot{\gamma} = \dot{\gamma}_0(T) \exp\left(-\frac{v_a \tau^*}{kT}\right)$$

where k is Boltzmann's constant, and the term $\dot{\gamma}_0(T)$ expresses the energy of activation and the effect of the temperature on the micro-structure (G'sell and Jonas, 1981). The expression for the apparent volume of activation may now be derived:

$$v_a = kT \left(\frac{\partial \ln \dot{\gamma}}{\partial \tau}\right)$$

Since $m = \frac{\partial \ln \tau}{\partial \ln \dot{\gamma}} = \frac{\partial \tau}{\tau \partial \ln \dot{\gamma}}$, the expression can be rewritten as:

$$v_a = \frac{kT}{m\tau}.$$

In the present study on attempt will be made to obtain an additive form of the constitutive equation since a simple multiplicative form is already available. However, the concept of apparent volume of activation may still be applied and in the case of polycarbonate deformed in simple shear at ambient temperature, $v_a = 4700\ A^{03}$. A simple calculation using the density and the molecular weight of a monomer indicates that this volume corresponds to about 15 polycarbonate monomers.

Plastic Deformation Model

BRIEF REVIEW OF THE MODELS OF PLASTIC DEFORMATION

Among the models of plastic deformation which have been proposed for glassy amorphous polymers, Robertson's model (1966) was the first plausible one. Robertson considers the existence of two different macromolecular configurations with different energies which result from the rotation of the molecular chain segments about a covalent bond. The application of an external stress increases the population of the configuration which corresponds to the activated state at the expense of the lower energy configuration (see Figure 24a).

The elastic limit is attained when the population of the activated state becomes equal to that which could be found if the polymer where in the molten state. This assumption, coupled with the WLF (Williams, Landel and Ferry) equation (J.D. Ferry, 1961) enables the calculation of the theoretical elastic limit at different temperatures. This model is in agreement with experimental data obtained at temperatures around T_g for low strain rates (Robertson, 1966; Argon and Bessonov, 1977a). Experimentation has also confirmed the increase in the 'cis' (activated state) configuration (Theodorou, 1982 cited by Lefebvre, 1982). Among the shortcomings of this model, however, are its inability to predict the plastic behavior of glassy polymers at low temperatures and its inability to explain the transitory effects due to change in strain rate. Because of the statistical distribution of the bonds in a polymer, this model predicts that the mechanism of deformation is homogeneous. However, it still contains arguments for the existence of "nuclei" of plastic deformation or microscopic defects.

The theoretical elastic limit for slip along entire planes was calculated by Frenkel (1926) for crystalline materials and modified by Bowden and Raha (1974) for application to glassy amorphous polymers. The calculated value ranges from 0.1 to 0.5 G where G is the elastic shear modulus of the material. For all materials, the experimentally determined values of the elastic limit are very much lower than the calculated values, from 10^{-4} to 10^{-2} G for crystals (Friedel, 1964) and from 10^{-2} to 10^{-1} G for polymers (Whitney and Andrews, 1967). This discrepancy resulted in the development of the dislocation theory for crystalline materials, while for amorphous polymers, models with microscopic defects have been proposed.

For Argon (1973; Argon and Bessonov, 1977a and b) these defects are intramolecular defects in the form of disclination pairs (Li, 1982) which nucleate on the molecular chain (Figure 24b). The polymer is considered as a group of smooth molecular chains with an isotropic initial distribution of the molecular chain orientations. The applied stress favors the nucleation of disclination pairs by lowering the free energy of formation to a free enthalpy which can be readily supplied by thermal fluctuations. The calculations of the model are based on the energy of formation of a disclination derived previously by Li and Gilman (1970), modified by taking the molecular interactions into consideration. The model agrees quite well with experimental results at low temperatures (Argon, 1973; Argon and Bessonov, 1977a and b) but fails to account for the polymer response at high temperatures (near T_g) which is the range of applicability of Robertson's model (Argon and Bessonov, 1977a). At O°K, the disclination pair model predicts a single yield stress value for all polymers, $\tau y = (1 - \nu) / G$ which is not verified by extrapolation based on experimental data (Argon and Bessonov, 1977a and b). A modification of the theory which takes the structural differences of different polymers into account could lead to a better correlation between theory and experimental results (Argon and Bessonov, 1977a).

Other difficulties associated with Argon's model include the rather arbitrary selection of the frequency at which the shear modulus is obtained and the artificial adjustment of parameters (Lefebvre, 1982). The equations of the model are also relatively complicated and do not allow an immediate correlation between the physical mechanisms and the theoretical aspects of the model.

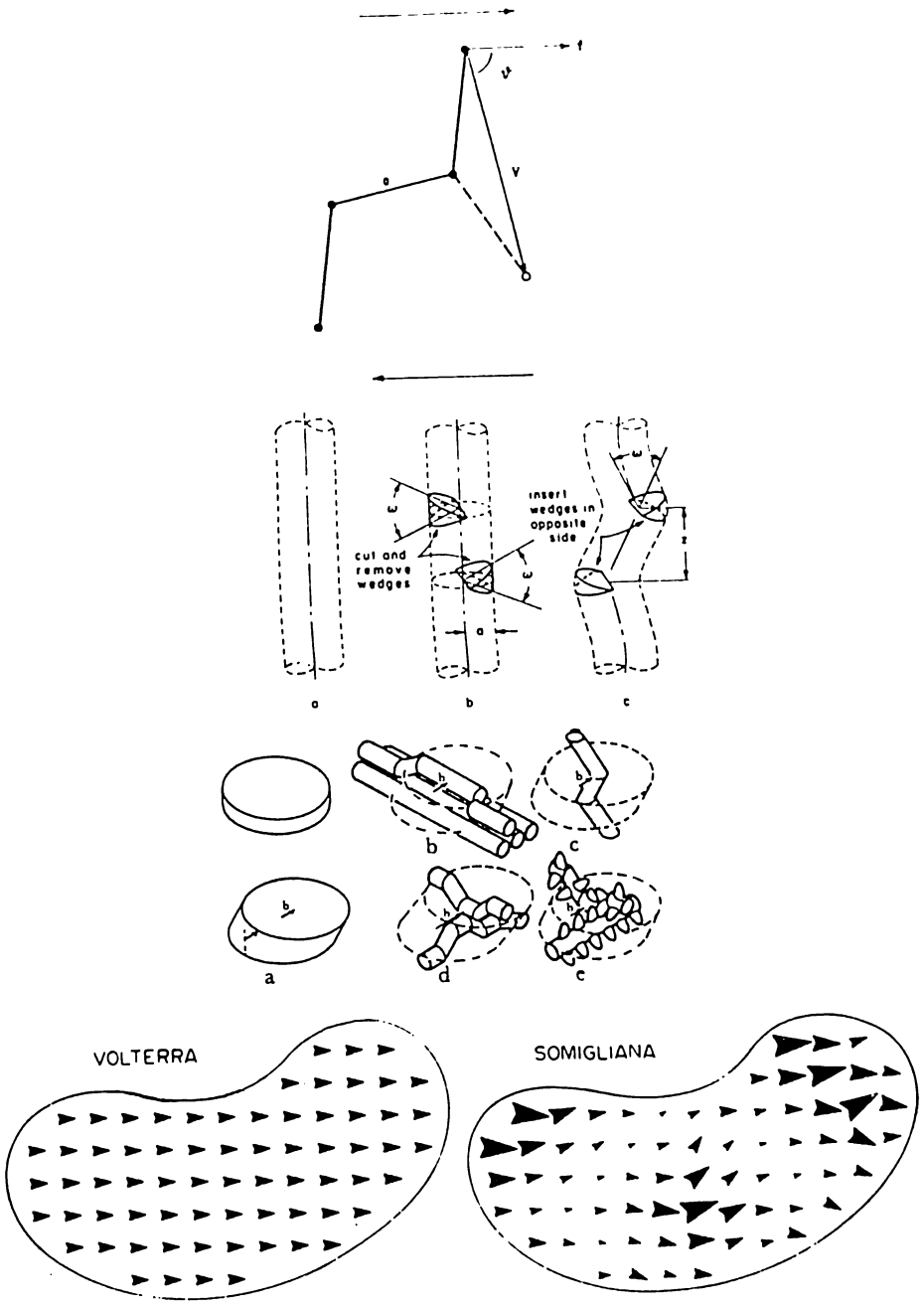

Figure 24: Elements of the plastic deformation models for glassy amorphous polymers

For Bowden and Raha (1974) the elementary defects are envisaged as dislocation loops which delimit sheared zones (Figure 24c). These authors adopt Gilman's (1973) point of view that the notion of a dislocation in an amorphous material is acceptable. In their analysis, the equivalent Burger's vector b is defined as an elementary shear displacement in the area occupied by the defect. The calculations are then based on dislocation theory with the energy of nucleation of a dislocation loop as the main component of the energy barrier. The external applied stress reduces the height of this barrier and the elastic limit is attained once the barrier has been reduced to a value comparable to the available thermal energy. This model predicts the behavior of some amorphous polymers rather well (Bowden and Raha, 1974; Thierry et. al., 1974).

The concept of a dislocation in an amorphous solid presents some problems regarding its topology considering that long range disorder characterizes a typical amorphous "structure."

Li (1976 and 1982) suggests that the classical Volterra dislocation model may be replaced by the concept of Somigliana dislocation which, unlike the former concept, incorporates the possibility of the fluctuation of Burger's vector along the dislocation line (Figure 24d). Considering the uncertainties regarding the nature of the defects, it is not surprising that Argon's and Bowden and Raha's models give different results for the same polymer. It would seem, however, that the latter theory would have "internal" inconsistencies (Kramer, 1975).

In a recent computer simulation study, Vitek (1982) and Srolovitz et. al. (1981) analyzed the topology of the elementary mechanisms of plastic deformation in a three-dimensional model of an amorphous monoatomic material. Results indicate that plastic flow is accompanied by the multiplication of microscopic zones which contain a local shear stress concentration. These "τ defects" as called by the authors, do not affect the density of the material but favor the continuation of the plastic flow. No simulation of the same type has yet been done for glassy polymers but it would seem that the concept of a local disturbance leading to easy shear is not unreasonable in an macromolecular amorphous substance.

Escaig (1982) and Lefebvre (1982) also use the concept of a localized microscopic defect in their attempt to apply the thermodynamics and kinetics of plastic flow in crystalline solids to glassy amorphous polymers. A nucleus of plasticity is viewed as a small volume of sheared material which forms due to thermal fluctuations. The experimental work associated with the model (Lefebvre, 1982) indicates the presence of two different deformation mechanisms:

(a) a thermally activated mechanism at low temperatures which is analogous to dislocation glide in crystalline solids.

(b) a high temperature diffusion-based mechanism with a constant activation energy which is apparently controlled by molecular migration.

The transition temperature T_c, between these two modes of deformation appears to correspond to the onset of the secondary (β) relaxation in the material.

Without precisely defining the nature of the defects, G'sell and Jonas (1981) assumes their existence in their analysis of the transitory behavior of polymers at the elastic limit due to changes in the strain rate. Their model assumes the existence of localized molecular misfits (or plastic waves) of linear character which nucleate and propagate under the action of the effective stress σ^*. This is also the stress component due to strain rate. Plastic deformation takes place at a given strain rate when the critical density of defects is attained. Using the hypothesis of Gilman and Johnston (Johnston, 1962), it can be shown that the speed at which the defects propagate changes instantaneously with the applied stress while the density of defects can only increase gradually as straining proceeds. A material which initially has no defects will then show a stress drop after yield because the high stress level is needed only to nucleate enough defects for the initiation of plastic deformation. Once the critical defect density is reached, plastic deformation continues at a lower stress level. This would explain the stress drops observed in the stress-strain curves of glassy amorphous polymers (Brown and Ward, 1968; Wu and Turner, 1973; G'sell and Jonas, 1979). In cases where the nucleation of defects cannot take place readily in the entire volume of the material, the critical density can be attained in certain areas by the movement and concentration of defects particularly where there are stress concentrations. This results in localized plastic deformation in the form of shear or deformation bands. These have actually been observed on numerous occasions in glassy amorphous polymers (Argon et. al., 1968; Bowden and Jukes, 1968; Bowden and Raha, 1970; Wu and Turner, 1973; Wu and Li, 1976). Transitory effects (such as those due to strain rate changes during deformation) can also be explained by this model. In a material already deforming at a given strain rate, a steady state defect density due to the strain rate is present. When there is a sudden increase in the strain rate, the defect speed instantaneously changes to match the new deformation rate while the density increases gradually. For the defect density to reach a new steady state value a higher stress needs to be applied and results in a stress over-shoot during the transitory period just after the strain rate changes. When the new defect

density is reached, the deformation continues at a stress level corresponding to that which would have been obtained if the test had started at the new strain rate. This interpretation agrees so far with experimental observations (G'sell and Jonas, 1981).

This review of the literature indicates that the concept of elementary defects as part of a plastic deformation mechanism is not a new one and is acceptable even for glassy amorphous polymers.

EXPERIMENTS INDIDCATING THE PROCESS AND INFLUENCE OF DEFECTS

A material which initially has no defects should have a high elastic limit, a stress drop at yield and exhibit localized plastic deformation. Annealed polycarbonate shows all of these characteristics at ambient temperature (see Figure 7). On the other hand, the presence of defects should be indicated by a lower elastic limit, the absence of a stress drop and macroscopically homogeneous plastic deformation. In crystalline solids it is now well-known that predeformation in the plastic range leads to the multiplication of microstructural defects. For polycarbonate, the mechanical response of previously deformed specimens can be explained by the presence of defects which are nucleated during the initial plastic deformation stage. Cyclic and reverse shear testings indicate that previously deformed specimens have a lower elastic limit and deform plastically without localized plastic strain (Curves 1 and 2, Figure 25). A specimen which is previously plastically deformed and then returned to a state of zero strain would still have a certain density of defects which leads to easier plastic deformation in its entire volume. The difference between the stress levels in cyclic and reverse shear tests would then be due to the difference in the signs of the defects with respect to the final shear direction. Plastic deformation seems to be easier in the same direction as the initial stress which formed the defects.

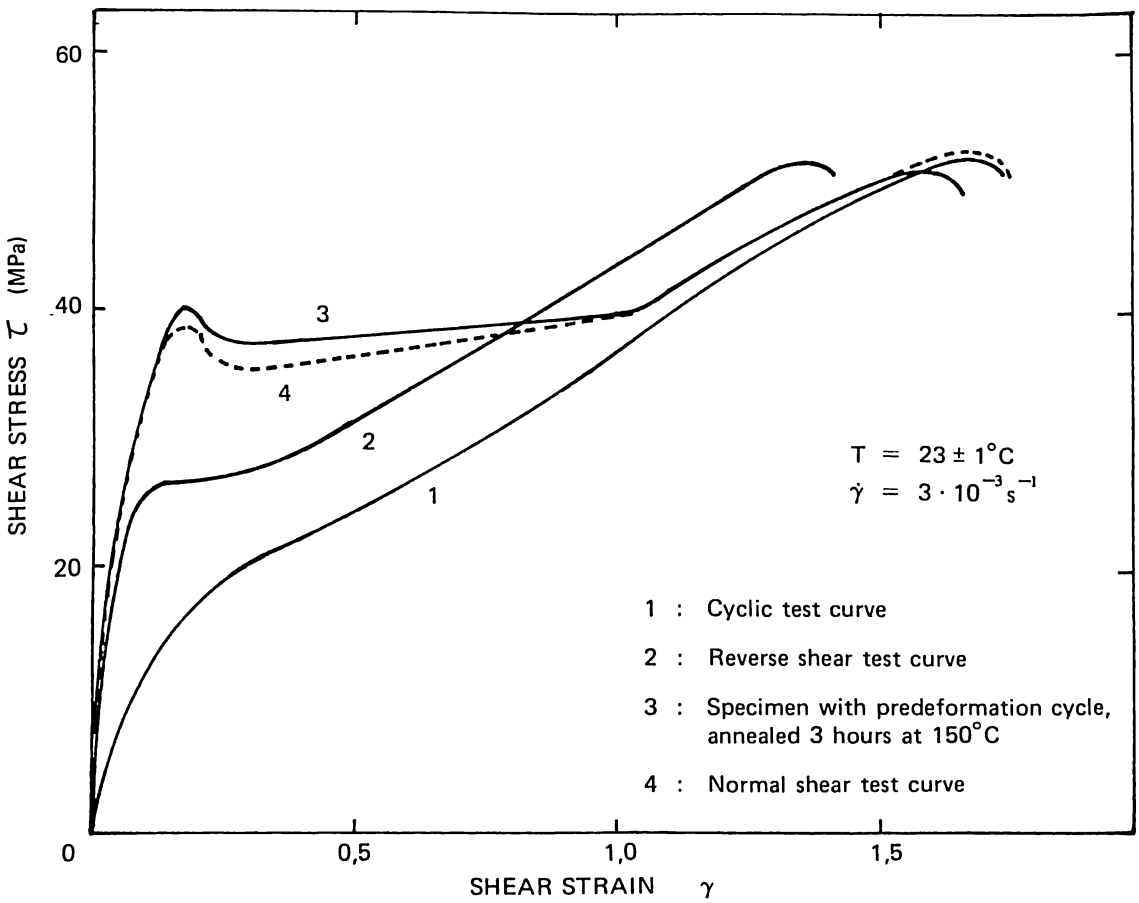

Figure 25: Shear test curves showing the influence of defects on the deformation behavior of polycarbonate

Annealing at temperatures close to T_g followed by slow cooling lead to the annihilation of defects. This treatment most probably relaxes and rearranges the molecular chains and erases any effects of a previous mechanical treatment. This is borne out by the results of a test carried out on a previously deformed and annealed specimen. Retesting gives a curve with a high elastic limit and a stress drop, indications that the plastic deformation becomes heterogenous once more.

The results of the low frequency fatigue test also indicate the presence of defects (see Figure 20). The first cycle shows a high elastic limit and a stress drop at yield while the succeeding cycles have lower and almost identical stress levels indicating the existence of a stable state.

The defects apparently form during the first cycle and the succeeding cycles are due to the stabilization of the defect density. The observations of Rabinowitz and Beardmore (1974) are in agreement with the results just presented. Low amplitude fatigue tests on polycarbonate and polymethylmethacrylate in the glassy state also showed a softening effect in the first few cycles followed by a stabilization of the recorded stress levels. These results were explained by the existence of defects: the defect density increases during the incubation period at the start of the test and eventually steady state is established when the necessary density is reached.

Relaxation during unloading also appears to lead to an annihilation of defects (G'sell and Jonas, 1981). The internal friction of a material is directly linked to the movement of defects produced during plastic deformation. Tensile tests conducted together with internal friction measurements on glassy polycarbonate showed internal friction to be a decreasing function of the relaxation time. The amount of internal friction returns to its value before relaxation when the deformation process is continued (Rafi, 1982). It would seem that defects created by plastic deformation are annihilated during mechanical relaxation and then renucleated when deformation is continued.

NATURE OF DEFECTS

In an attempt to differentiate between material supposedly containing defects and material without defects, density measurements were carried out on samples with different mechanical treatment histories. The measurements were carried out at 23°C with a water-sodium bromide specific gravity column (ISO R 1183). The results are shown in Table 1. It can be noted that the samples of material deformed in tension (PCE 3) and in shear (PC207, PC208) have a density which is 0.5 percent higher than undeformed (PCN, PCNT) or annealed material (PC 215). This result is in agreement with those obtained by other investigators (see Table 2). It, therefore, appears that plastic deformation makes a material more dense, and that it is the defect-containing material which is more dense. It is therefore not possible to speak of these defects as regions of high free volume, an idea already advanced by Rabinowitz and Beardmore (1974). Neither can crazes exist in the deformed material because their presence would have been manifested as a reduction in the density of the material, a case already observed in the deformation of polycarbonate film (Ishikawa et. al., 1976). In fact, it has already been shown that crazes are microfractures (and therefore empty space) whose inner surfaces are joined by fibrillar structures (Kramer, 1982).

Comparison of the Simple Shear Test Curve with the Tensile Test Curve

CHOICE OF CURVES FOR COMPARISON

Considering the differences in the stress fields due to the different testing methods it would seem possible to compare the different stress-strain curves by using the concepts of equivalent stress and equivalent strain. To accomplish this, expressions which can transform the shear response curve $\tau(\gamma,\dot{\gamma})$ into an equivalent response curve $\sigma_{eq}(\varepsilon_{eq}\dot{\varepsilon}_{eq})$ must be determined. In this study, an attempt to compare the shear test results with those of the tensile test will be done for the case of polycarbonate.

Table 1: Density measurements at 23 ± 1°C

Sample	Mechanical History	Density, g/cm^3
PCN	Undeformed polycarbonate	1.1974 ± 0.0013
PCNT	Undeformed polycarbonate Annealed 3 hours at 150°C Quenched in ice water	1.1970 ± 0.0013
PCE3	Tensile test specimen $\gamma_{pl} = 0.57$ $\dot{\varepsilon}_{nom} = 10^{-3}$ s^{-1} T = 23°C	1.2050 ± 0.0017
PC207	Shear test specimen $\gamma_{pl} = 0.77$ ($\varepsilon_{pl,eq} = 0.37$) $\dot{\gamma} = 3\ 10^{-3}$ s^{-1}, T = 23°C	1.2033 ± 0.0017
PC208	Shear test specimen Deformed to $\gamma_{pl} = 0.80$ and brought back to $\gamma = 0$ $\dot{\gamma} = 3\ 10^{-3}$ s^{-1}, T = 23°C	1.1997 ± 0.0017
PC215	Shear test specimen Deformed to $\gamma_{pl} = 0.80$ and brought back to $\gamma = 0$; Annealed 3 hours at 150°C Cooled slowly to room temperature	1.1972 ± 0.0017

Table 2: Increase in specific gravity due to plastic deformation.

Polymer Tested*	Type of Test	Increase in Specific Gravity	Reference
PC	Tensile Test 25°C	0.20%	Brady and Yeh, 1971
PMMA	Tensile Test 25°C	0.50%	Brady and Yeh, 1971
PS, atactic	Tensile and Compression 25°C	0.25%	Brady and Yeh, 1971
PC	Fatigue 25°C	1%	Rabinowitz and Beardmore, 1974
PC	Torsion 21°C	0.1%	Wu and Turner, 1973
PMMA	---	0.5%	Enders, 1969 cited by Brady and Yeh, 1971

* PC = polycarbonate; PMMA = polymethylmethacrylate; PS = polystyrene.

For comparison, the shear stress-shear strain curve obtained through cyclic testing is a better choice than the curve for an annealed specimen because the cyclic test curve represents the intrinsic shear response of polycarbonate. It is to be recalled that the cyclic test curve is free from transitory and geometry (i.e., necking) effects (see Figure 26).

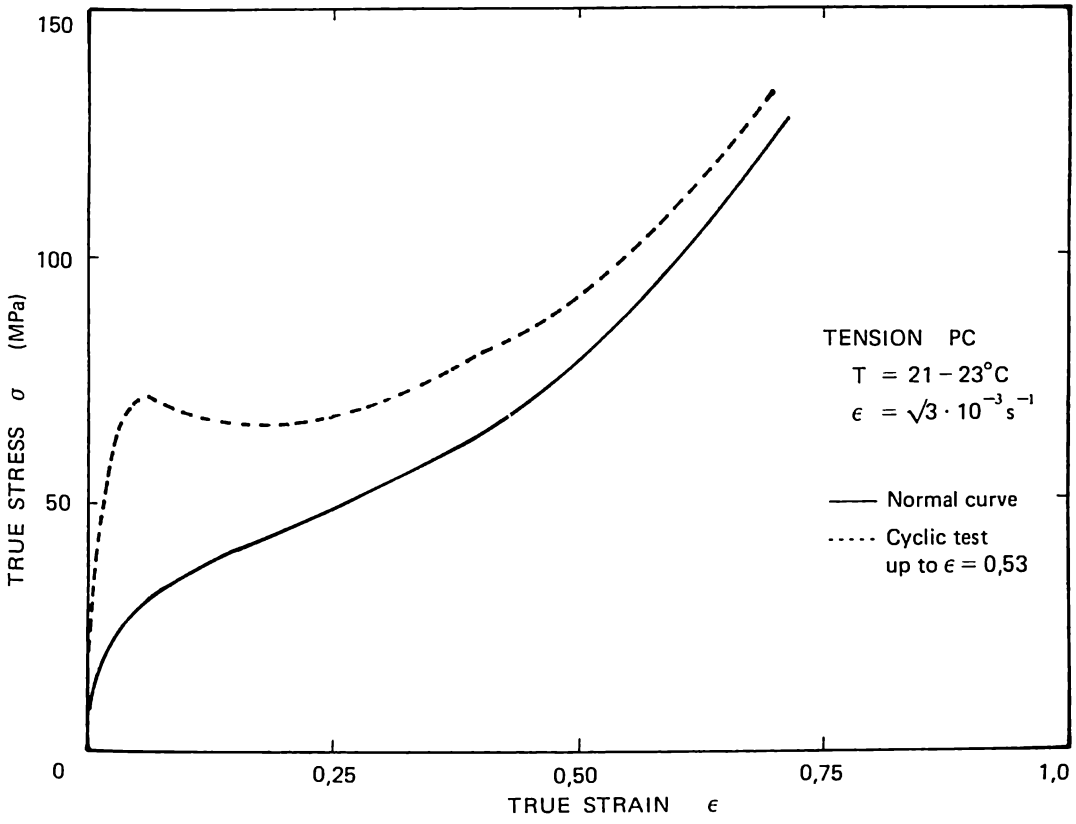

Figure 26: Shear test curves

In choosing the tensile test curve, true stress-true strain curves were used to remove the effects of necking on the material response. Cyclic testing was also done to ascertain if there was also a difference in the curves. Figure 27 shows results similar to those obtained in shear. The cyclic tensile test curve was therefore chosen.

The two curves chosen for comparison have the same general appearance. Both have an initial viscoelastic stage with steep slopes, a gradual slope change at the elastic limit and a slightly increasing strain hardening coefficient after yield. At large strains however, the strain hardening coefficient seems to stabilize at a certain value for the shear curve while it increases rapidly for the tensile curve.

EQUIVALENT STRAIN

Equivalent strain defines the generalized state of strain of a given system. Uniaxial tension is a special case and the equivalent strain expression is identical to the true strain, $\mathcal{E} = \ln(L/L_0)$.

A general approach is to use the second invariant of the strain tensor to obtain an expression for the equivalent strain:

$$\varepsilon_{eq} = \frac{2}{\sqrt{3}} \left[\left\{ (\varepsilon_{11} - \varepsilon_{22})^2 + (\varepsilon_{22} - \varepsilon_{33})^2 + (\varepsilon_{11} - \varepsilon_{33})^2 \right\} /6 + (\varepsilon_{12}^2 + \varepsilon_{23}^2 + \varepsilon_{31}^2) \right]^{1/2}$$

For large strains, Eichinger and Siebel (1955) derived a logarithmic equivalent strain equation for shear:

$$\varepsilon_{eq} = \frac{2}{\sqrt{3}} \ln \left[\frac{1}{2} \left(\gamma + \sqrt{\gamma^2 + 4} \right) \right]$$

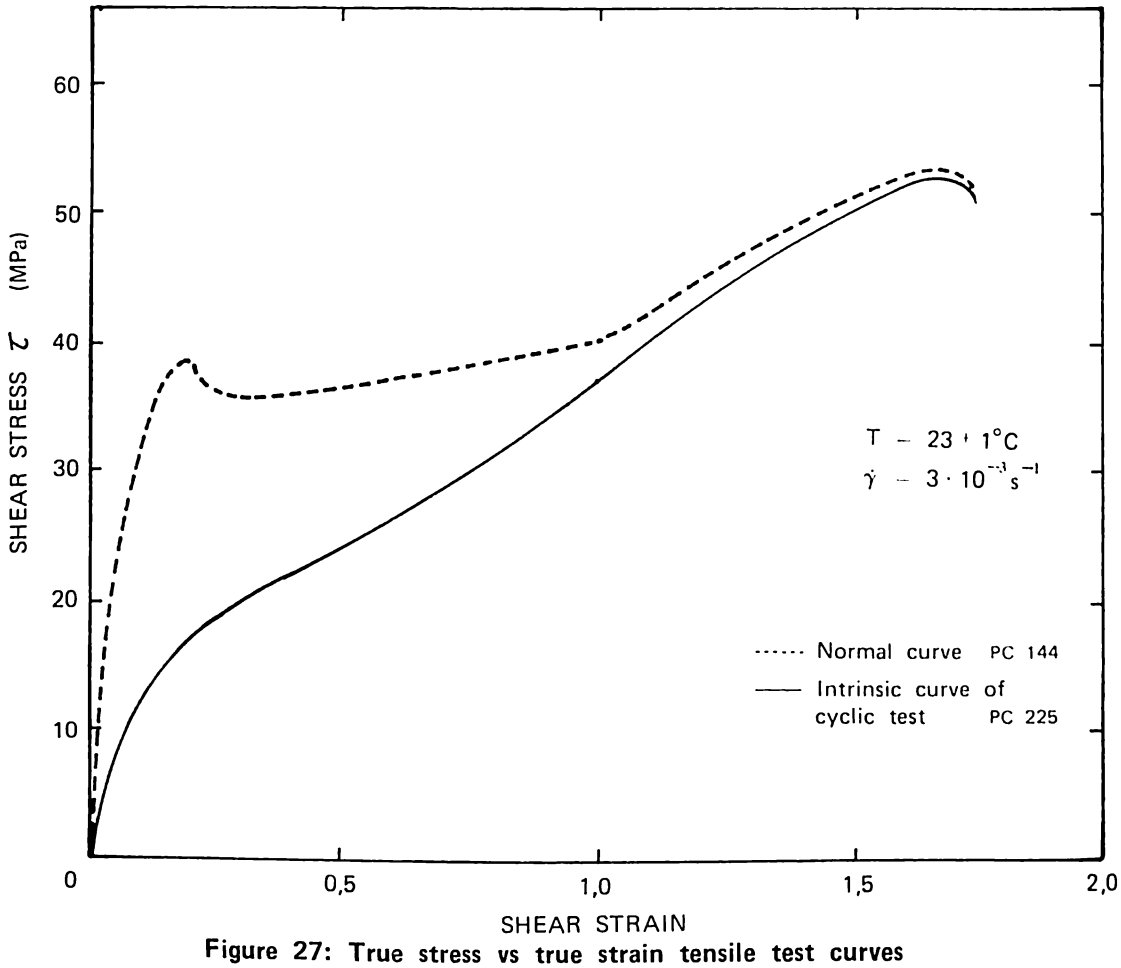

Figure 27: True stress vs true strain tensile test curves

Equivalent states of strain for tension and shear as considered by Eichinger and Siebel also correspond to equivalent macromolecular orientations. Using the orientation factor gives an $\varepsilon_{eq} - \gamma$ curve which coincides with that obtained using the Eichinger-Siebel expression (Gopez, 1983).

Shrivastava et. al. (1982) proposed another approach to the obtention of equivalent strain for simple shear using a remark made by Zener and Hollomon (1944). At large strains, the principal strain axes rotate as shearing takes place and the expression for ε_{eq} must be obtained by integrating the increment $d\varepsilon_{eq}$ along the deformation path. This calculation was carried to completion by Canova et. al., (1982) and results in the expression: $\varepsilon_{eq} = \gamma/\sqrt{3}$

Values obtained with this expression at high strains are larger than those obtained by the Eichinger-Siebel expression. In the strain range covered by the tests in this study however, the different expressions for ε_{eq} give approximately the same values.

EQUIVALENT STRESS

The equivalent stress may be calculated by using the concepts associated with plasticity criteria. According to Tresca's criterion (Dieter, 1976), plasticity is initiated when the

maximum shear stress in the material attains a certain critical value. In uni-axial tension, $\tau_c = \sigma_0/2$ with σ_0 being the yield stress. Using Tresca's concept, two systems will have equivalent states of stress if they have the same maximum shear stress. For a shear test, the stress equivalent to a shear τ is therefore: $\sigma_{eq} = 2\tau$. Tresca's criterion does not take hydrostatic pressure effects into consideration. Modifications have been done using the Mohr-Coulomb criterion or the Drucker-Prager calculation (see for example Li and Wu, 1976). These expressions will not be considered in this discussion because the situation remains unresolved and subject to discussion.

The Von Mises criterion proposes that plasticity starts when the stored elastic energy reaches a critical value. This is expressed mathematically by the second invariant of the stress tensor:

$$J_2 = \left[(\sigma_1 - \sigma_2)^2 + (\sigma_2 - \sigma_3)^2 + (\sigma_3 - \sigma_1)^2 \right]$$

where $\sigma_1, \sigma_2, \sigma_3$ are the principal stresses. According to this criterion, two systems will have equivalent stress states if J_2 has the same value in both systems. The equivalent stress is then expressed as:

$$\sigma_{eq} = \frac{1}{\sqrt{2}} \left[(\sigma_1 - \sigma_2)^2 + (\sigma_2 - \sigma_3)^2 + (\sigma_3 - \sigma_1) \right]^{1/2}$$

In simple shear, $\sigma_1 = -\sigma_2$ and $\sigma_3 = 0$ and the expression reduces to: $\sigma_{eq} = \sqrt{3}\,\tau$.

Equivalent stresses calculated by the preceding expression are 15 percent lower than those obtained using Tresca's criterion.

COMPARISON OF EQUIVALENT CURVES

Since it is not possible to reject or argue convincingly against any of the previously cited expressions for equivalent stress and strain, the possible combinations were instead taken into consideration in establishing the equivalent curve for shear. The shear curve should lie in the region described by the two extreme curves represented in Figure 28.

Curve No.	ε_{eq}	σ_{eq}
1	$\gamma / \sqrt{3}$	$\sqrt{3}\tau$
2	$(2/\sqrt{3})\ \ln \left[\frac{1}{2} (\gamma + \sqrt{\gamma^2 + 4}) \right]$	2τ

It is to be noted that the reference shear strain rate $\dot{\gamma}_3 = 3\ 10^{-3}\ s^{-1}$ was chosen such that it would be equivalent to the tensile strain rate $\dot{\varepsilon} = 3\ 10^{-3}\ s^{-1}$ used for the tensile tests.

A look at Figure 28 indicates that the equivalent curves for shear and tension are very close to each other for strains lower than $\Sigma_{eq} = 0.5$. These results confirm those obtained by Boni (1981) in the case of polyethylene, that the tensile test curve passes above the shear curve at larger strains. This divergence has also been noted for copper (Canova et. al., 1982; Gil-Sevillano and Aernoudt, 1975) but the stress level difference is much smaller than that for polymers. In the case of metals, this divergence between curves has been attributed to dislocation glide on fewer non-intersecting planes in simple shear. Consequently, shear testing shows less strain hardening.

For amorphous polymers the problem is less straightforward because the elementary deformation mechanisms are not as well known as they are for metals. Numerous observations indicate the existence of shear bands in polymers (Argon et. al., 1968; Wu and Li, 1976; Bowden and Raha, 1970). In tensile testing, the intersection of these deformation bands has also been demonstrated (Bauwens, 1967) while in simple shear, results of the present study show the formation of a single band parallel to the shear axis and the absence of band intersection. The formation and development of the deformation band for the different modes of deformation may explain the difference in the strain hardening behavior of the material.

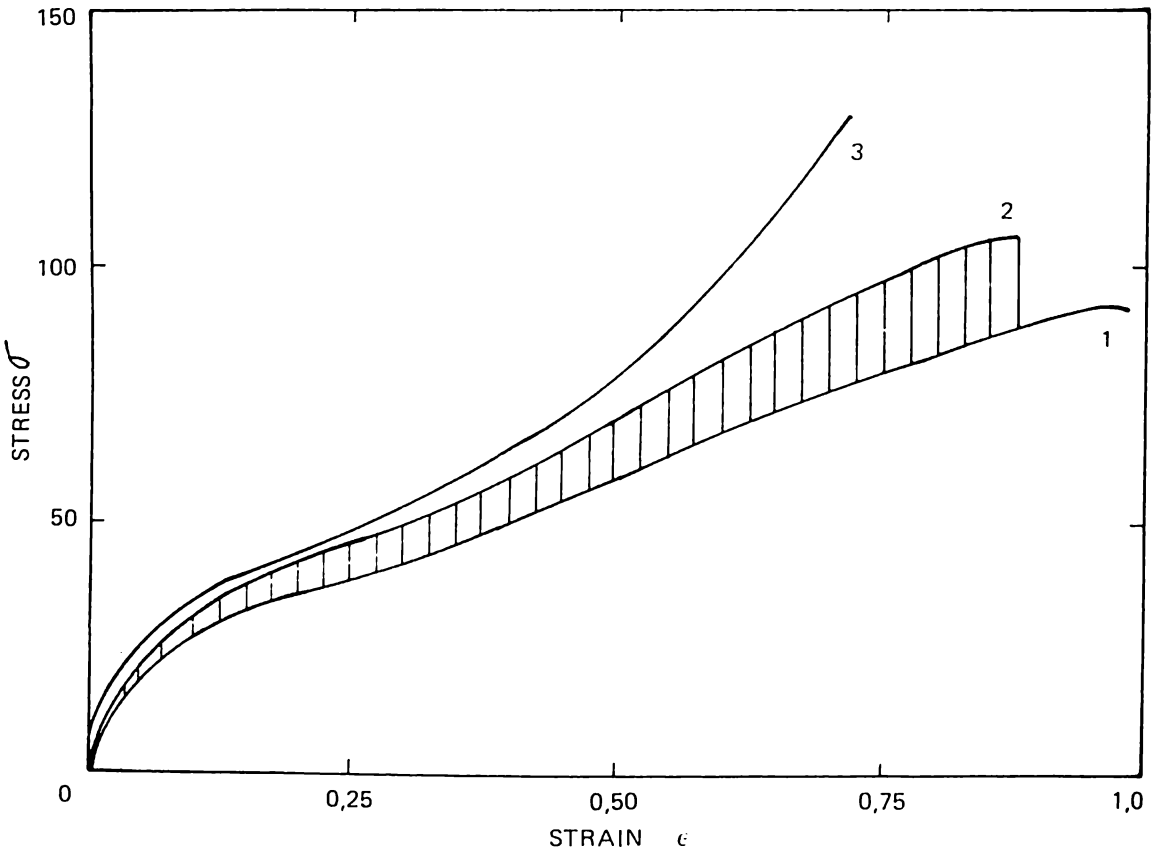

1 $\sigma_{eq} = \sqrt{3}\tau \; / \; \epsilon_{eq} = \gamma / \sqrt{3}$

2 $\sigma_{eq} = 2\tau \; / \; \epsilon_{eq} = (2/\sqrt{3}) \; \ell n \; [1/2 \; (\gamma + \sqrt{\gamma^2 + 4}) \;]$

3 $\sigma - \epsilon$ tensile test

Figure 28: Comparison of shear and tensile tests

SUMMARY AND CONCLUSIONS

The plane simple shear test developed by G'sell and Boni was applied to the case of bisphenol A polycarbonate, an amorphous polymer with glassy characteristics up to T_g = 145°C. From shear tests carried out at different temperatures and strain rates, an empirical constitutive flow equation of the multiplicative type was obtained. During the tests it was observed that plastic deformation was concentrated in a shear band which forms at the yield point. This shear band is unaffected by geometrical effects such as reduction of cross-sectional area.

A plastic predeformation cycle modifies the mode of deformation of polycarbonate without an apparent effect on the macroscopic characteristics of the material.

An analysis of the results resulted in the proposition that plastic deformation is a thermally activated process which depends on the nucleation and propagation of microscopic defects. The exact nature of these defects was not determined but a defect may be viewed as a sheared area with a plastic deformation gradient.

At present, it seems that tensile tests and shear tests cannot yet be derived from each other using an analysis based solely on the concepts of equivalent stress and strain. It is necessary to obtain a deeper knowledge of the elementary deformation mechanisms and the possible interactions of these mechanisms before a valid system of generalized stress and strain for an amorphous polymer can be proposed.

REFERENCES

1. Aly-Helal N.A. (1982). "Etude et Simulation du Developpemend de la Striction dan le Polyethylene a Haute Densite", Thesis Docteur-Ingenieur. I.N.P.I. Nanoy. France.
2. Argon A.S., Andrews R.D., Godrick J.A. and Whitney W. (1968). Appl. Phys. *39*, 1899.
3. Argon, A.S. (1973), Phil. Mag., *28*, 839.
4. Argon A.S. and Bessonov M.I. (1977) A, Phil. Mag., *35*, 917.
5. Argon A.S. and Bessonov M.I. (1977) B, Polym. Eng'g. and Sci. *17*.
6. Atkin R.J. and Fox N. (1980), "An Introduction to the Theory of Elasticity", Longman.
7. Bauwens J.C. (1967), J. Polym. Sci. A-2, 5, 1145.
8. Bauwens-Crowet C., Bauwens J.C. and Homes G. (1972), J. Mater. Sci, *7*, 176.
9. Bauwens-Crowet C, Ots J.M. and Bauwens J.C. (1974), J. Mater. Sci. *9*. 1197.
10. Boni S. (1981), "Conception d'une Machine de Cisaillement Plan pour la Determination du Comportement Plastique de Materiaux Polymeres," Thesis-"Ingenieur C.N.A.M." Nancy, France.
11. Boni S. G'Sell C., Weynant T.E. and Haudin J.M. (1982), Polymer Testing, *3*, 3.
12. Bowden P.B. and Jukes J.A. (1968), J. Mater. Sci., *3*, 1833.
13. Bowden P.B. and Raha S. (1970), Phil. Mag., *22*,463.
14. Bowden P.B. and Raha S. (1974), Phil. Mag., *29*, 149.
15. Brady T.E. and Yeh G.S.Y. (1971), J. Appl. Phys., *42*, 4622.
16. Brown N., Duckett R.A. and Ward I.M. (1968), Phil. Mag., *18*, 483.
17. Brown N. and Ward I.M. (1968), J. Polym. Sci. A-2, *6*, 607.
18. Canova G.R., Shrivastava S., Jonas J.J.and G'Sell C. (1982). "The Use of Torsion Testing to Assess Material Formability" in "Formability of Metallic Materials-2000 A.D.", ASTM STP 753, J.R. Newby and B.A. Niemeler ed., American Society for Testing and Materials, p. 189.
19. Cornes P.L. Smith K. and Haward R.N. (1977), J. Polym. Sci., *15*, 955.
20. Dieter G.E. (1976), "Mechanical Metallurgy," 2nd ed., McGraw-Hill Book Company, New York.
21. Eichinger A. and Siebel A. (1955), "Handbuch der Werktoffprufung." Zwelte Auflage, Springer-Verlag, Berlin.
22. Enders D.H. (1969), Polymer Preprints ACS, New York, *10*, 1132, cited by Wu and Turner (1973).
23. Escaig B. (1982),"Kinetics and Thermodynamics of Plastic Flow in Polymeric Glasses" in "Plastic Deformation of Amorphous and Semi-Crystalline Materials", B, Escaig and C G'Sell ed., Editions de Physique, p. 187.
24. Escaig B. and G'Sell C. (1982), editors, "Plastic Deformation of Amorphous and Semi-Crystalline Materials", Editions de Physique.
25. Eyring H. (1936), J. Chem. Phys., *4*, 283.
26. Ferry J.D. (1961), "Viscoelastic Properties of Polymers", John Wiley and Sons, Inc., New York.
27. Fotheringham D.G. and Cherry B.W. (1978), J. Mater. Sci., *13*, 231 and 951.
28. Frenkel J. (1926). Z. Phys., *37*, 572.
29. Friedel J. (1964), "Dislocations", Pergammon Press, Oxford.
30. Gilman J.J. (1973), J. Appl. Phys., *44*, 675.

31. Gil-Sevillano J. and Aernoudt E. (1975), Met. Trans. A, *6A*, 2163.

32. Gopez A.J.R. (1983) "Etude de la Deformation du Polycarbonate en Cisaillement Simple", Thesis-"Docteur-Ingenieur", I.N.P.I., Nancy, France.

33. G'Sell C. and Jonas J.J. (1979), J. Mater. Sci., *14*, 583.

34. G'Sell C. and Jonas J.J. (1981), J. Mater. Sci., *16*, 1956.

35. G'Sell C., Boni S. and Shrivastava S. (1983), J. Mater. Sci., *18*, 903.

36. G'Sell C., Aly-Helal N.A. and Jonas J.J. (1983) B to be published.

37. Heijboer J. (1969), Br. Polym. J., *1*, 3.

38. Heijboer J. (1977), Intern. J. Polymeric Mater., *6*, 11.

39. Ishikawa M., Narisawa I. and Ogawa H. (1976), Polym. Journal, *8*, 391.

40. Johnston W.G. (1962), J. Appl. Phys., *33*, 2716.

41. Kakudo M. and Kasai N. (1972), "X-ray Diffraction by Polymers", Kodansha Ltd., Tokyo.

42. Kramer E.J. (1975), J. Polym. Sci., Polym, Phys. Ed., *13*, 509.

43. Kramer E.J. (1982), "Crazing" in Plastic Deformation of Amorphous and Semi-Crystalline Materials", B. Escaig and C. G'Sell ed, Edition de Physique.

44. Lefebvre J.M. (1982), "Sur la Deformation Non-elastique des Polymeres Amorphes a l'Etat Vitreux", Thesis-"Docteur es Sciences, Physiques", Universite des Sciences et Techniques de Lille.

45. Li J.C.M. and Gilman J.J. (1970), J. Appl. Phys., *41*, 4248.

46. Li J.C.M. (1976), "Micromechanisms of Deformation and Fracture in Metallic Glasses" in "Metallic Glasses", ASM, p. 227, seminar 1976, published 1978.

47. Li J.C.M. and Wu J.B.C. (1976), J. Mater. Sci., *11*, 446.

48. Li J.C.M. (1982), "Dislocation Theory" and "Internal Stresses" in "Plastic Deformation of Amorphous and Semi-Crystalline Materials", B. Escaig and C. G'Sell ed., Editions de Physique.

49. Miles D.C. and Briston J.H. (1965), "Technologie des Polymeres", traduction franchise 1960, Dunod, Paris.

50. Rabinowitz S. and Beardmore P. (1974), J. Mater. Sci., *9*, 81.

51. Rafi O. (1982), "Etude de la Deformation du Polycarbonate a l'Etat Vitreux par Traction et Mesure du Frottement Interieur", Thesis-"Troisieme Cycle", E.N.S.M.A. Poitiers, France.

52. Robertson R.E. (1966), J. Chem. Phys., *44*, 3950.

53. Robertson R.E. and Joynson C.W. (1966), J. Appl. Phys., *37*, 3969.

54. Robertson R.E. and Joynson C.W. (1968), J. Polym. Sci., A-2, *6*, 607.

55. B. de Saint Venant (1856), "Memoires presentes par divers savants a l'Academie de l'Institut Imperial de France et imprimes par son ordre, Sciences Mathematiques et Physiques, Tome 14, Paris, p. 233-560.

56. Srolovitz D., Maeda K., Vitek V. and Egami T. (1981), Phil. Mag., *A44*, 847.

57. Theodorou M., Jasse B. and Monnerie L. (1982), Polymer, cited by Lefebvre (1982).

58. Thierry A., Oxborough R.J., and Bowden P.B. (1974), Phil. Mag., *30*, 527.

59. Turner S. (1973), "Creep in Glassy Polymers" in "The Physics of Glassy Polymers", R.N. Haward ed., Applied Science Publishers, London, p. 265.

60. Vitek V. (1982), "Atomic Structure and Defect in Metallic Glasses" in "Plastic Deformation of Amorphous and Semi-Crystalline Materials", B. Escaig and C. G'Sell ed., Editions de Physique, p. 143.

61. Ward I.M. (1970), J. Mater, Sci., 1397.
62. Whitney W. and Andrews R.D. (1967), J. Polym, Sci., *C61*, 2981.
63. Wu J.B.C. and Li J.C.M. (1976), J. Mater, Sci., *11*, 434.
64. Wu W. and Turner A.P.I. (1973), J. Polym. Sci., Polym. Phys., Ed., *11*, 2199.
65. Zener C. and Hollomon J.H. (1944), Trans. ASM. *33*, 168.